iScience

CellPress
OPEN ACCESS

Article

Cytokine-like-Vago-mediated antiviral response in *Penaeus monodon* via IKK-NF-κB signaling pathway

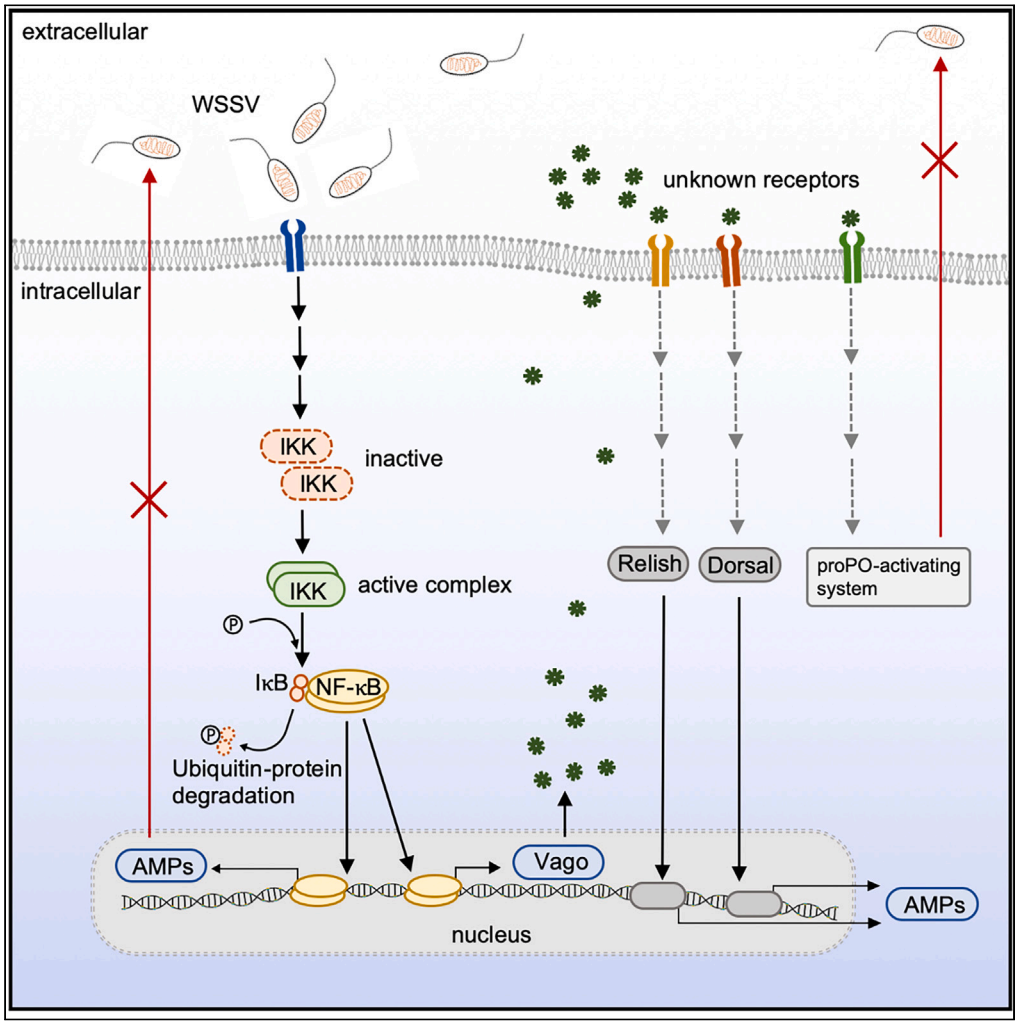

Zittipong Nanakorn, Taro Kawai, Anchalee Tassanakajon

anchalee.k@chula.ac.th

Highlights

WSSV induced Vago accumulation in area of hemocyte membrane and granules

Vago1 and *Vago4* RNAi increased shrimp cumulative mortality and WSSV replication

Vago associated with gene transcription in Toll, IMD, JAK/STAT pathways, and PO system

Vago1 and Vago4 stimulated NF-κB homologs Dorsal and Relish via IKK-NF-κB cascade

Nanakorn et al., iScience 27, 110161
July 19, 2024
https://doi.org/10.1016/j.isci.2024.110161

iScience

CellPress
OPEN ACCESS

Article

Cytokine-like-Vago-mediated antiviral response in *Penaeus monodon* via IKK-NF-κB signaling pathway

Zittipong Nanakorn,[1] Taro Kawai,[2] and Anchalee Tassanakajon[1,3,*]

SUMMARY

Interferon (IFN) system is the primary mechanism of innate antiviral defense in immune response. To date, limited studies of IFN system were conducted in crustaceans. Previous report in *Penaeus monodon* demonstrated the interconnection of cytokine-like molecule Vago and inhibitor of kappa B kinase-nuclear factor κB (IKK-NF-κB) cascade against white spot syndrome virus (WSSV). This study further identified five different *PmVago* isoforms. Upon immune stimulation, *PmVagos* expressed against shrimp pathogens. *PmVago1*, *PmVago4*, and *PmVago5* highly responded to WSSV, whereas, *PmVago1* and *PmVago4* RNAi exhibited a rapid mortality with elevated WSSV replication. Suppression of *PmVago1* and *PmVago4* negatively affected proPO system, genes in signal transduction, and AMPs. WSSV infection additionally induced *Pm*Vaog4 granule accumulation and cellular translocation to the area of cell membrane. More importantly, *PmVago1* and *PmVago4* promoters were stimulated by *Pm*IKK overexpression; meanwhile, they further activated *Dorsal* and *Relish* promoter activities. These results suggested the possible roles of the cytokine-like *PmVago* via IKK-NF-κB cascade against WSSV infection.

INTRODUCTION

The interferon (IFN) system in vertebrates is characterized by induction of IFNs that mediate the subsequent establishment of the cellular responses to invading pathogens. IFN molecules are a group of secreted cytokines with activities to respond against viral replication and regulate the function of immune cells.[1,2] In mammals, three types of IFNs (type I, II, and III) have been identified, all exhibiting significant antiviral activities.[3,4] IFN production occurring in various cells in response to viral infection and modulated by the interferon regulatory factors (IRFs) is considered to be central to the antiviral innate immunity in vertebrates.[4] Recently, complete genome sequences of *Drosophila melanogaster*[5] and *Anopheles gambiae* mosquito[6] predicted several parts of interferon-based antiviral system analogous to vertebrates. Study focusing on IFN analogous functions also found a number of antiviral molecules in tissue of the blue crab and crayfish. These observations are partially consistent with the presence of IFNs and IRFs that led to the upregulation of interferon-stimulated genes (ISGs) in vertebrates.[7] However, limited data concerning antiviral mechanism were reported for cytokine-like Vago in crustacea including shrimp.

In invertebrates, the innate immune system is stimulated when the pathogen-associated molecular patterns (PAMPs) are recognized by pattern recognition receptors (PRRs) such as Toll-like receptors (TLRs), retinoic acid-inducible gene-I (RIG-I)-like receptors (RLRs), NOD-like receptors (NLRs), C-type lectin receptors (CLRs), or cytosolic DNA sensors.[8–10] The PAMP recognition induced cellular and humoral immune responses through the recruitment of immune molecules aiming to combat the invasion. The various immune signaling of host defense mechanisms therein are stimulated, such as Toll, immune deficiency (IMD), JAK/STAT, and inhibitor of kappa B kinase-nuclear factor κB (IKK-NF-κB) signaling pathways.[11,12] The pathways were initiated on the basis of pathogen signature molecule recognition and respond through the production of antimicrobial peptides (AMPs).[9,13] Interestingly, the IKK-NF-κB pathway was considered as one of the signaling hub that functions in pathway cross-talking and is related to cytokine-like system in crustacean.[14,15] In vertebrates, the PAMP-stimulated PRRs triggered the IKK-NF-κB pathway cascade. Previous data demonstrated the essential role of the IKK-NF-κB pathway in coordinating the expression of type I interferons (IFNs), pro-inflammatory cytokines, and chemokines in mammals.[12] Recently, two inhibitors of kappa B kinases (IKKβ and IKKε) from black tiger shrimp *Penaeus monodon* were reported for affecting the transcription of the cytokine-like Vago. The results revealed the potential roles of *Pm*IKKs in shrimp antiviral response with the cytokine-like system through *Pm*Vago.[16] Study in Pacific white shrimp, *Litopenaeus vannamei* further revealed the activation of Vago gene (*Lv*Vago) by IFN regulatory factor (*Lv*IRF) in reporter gene assays.[3] The expression of Vago was induced by Vp_{AHPND} in *Penaeus vannamei*[17] and secreted as an interferon after viral infection in arthropods.[18] Following the activation, the elimination of invading viruses and bacteria commences by initiating innate and adaptive immune systems.[13,19]

[1]Center of Excellence for Molecular Biology and Genomics of Shrimp, Department of Biochemistry, Faculty of Science, Chulalongkorn University, Bangkok 10330, Thailand
[2]Laboratory of Molecular Immunobiology, Division of Biological Science, Graduate School of Science and Technology, Nara Institute of Science and Technology, Nara 630-0192, Japan
[3]Lead contact
*Correspondence: anchalee.k@chula.ac.th
https://doi.org/10.1016/j.isci.2024.110161

In addition to Vago, interferon β (IFNβ) and IFN regulatory factor 3/7 (IRF3/7) were characterized and regulated via NF-κB transcription factors in responses to different stimuli.[20] Besides, Dorsal and Cactus were the two NF-κB transcription factors promoting the circulating pro-inflammatory cytokines in fruit fly.[21] This suggested the significance of NF-κB signaling pathway against microbial infection through cytokine system. Therefore, Vago acting as an IFN-like molecule in shrimp antiviral response similar to the interferon from vertebrates is of a great interest.

Shrimp innate immune system including Vago and IκB kinase pathway in pathogen responses could be the key to understanding the unclear cytokine-like system. Here, we further identified five Vago isoforms from *Penaeus monodon*. They were characterized in correlation with IKK-NF-κB cascade and involved in immune responses against WSSV, a severe shrimp viral pathogen. *In vivo* transient RNA interference was performed to identify groups of immune-related genes and pathways affected following Vago transcript suppression and WSSV infection. Subsequently, the Vago's possible roles as the cytokine-like molecules in shrimp IKK-NF-κB cascade were determined by reporter assay. Specifically, these results offered the potential roles of Vago in shrimp antiviral response related to IKK-NF-κB cascade via IKK-NF-κB-Vago axis in cytokine-like system.

RESULTS

Cloning and sequence characterization of *PmVago*

The genomic DNA sequences of *PmVago* were obtained by *in silico* search and nucleotide BLAST program. The genomic scaffold sequences and genome organization showed that *PmVago1* (2,342 bp), *PmVago2* (2,756 bp), *PmVago3* (2,454 bp), *and PmVago5* (1,821 bp) were composed of three exons and two introns in varied lengths except *Pm*Vago4 that was observed in a 1,375-bp exon without intron. The cDNA sequences of *PmVago1*, *PmVago2*, *PmVago3*, *and PmVago5* contained start codons (ATG) located in exon 1 and stop codons (TAA or TGA) in exon 3, whereas a TAA stop codon of *PmVago4* was located in exon 1 (Figure 1A).

The full-length cDNA sequences of *PmVago1-5* were obtained by polymerase chain reaction (PCR) amplification using specific primers (Table S1) based on *L. vannamei Vago* and *P. monodon* reference genomes. Five isoforms of *PmVago* were identified and sequenced, including *PmVago1*, *PmVago2*, *PmVago3*, *PmVago4*, and *PmVago5* (Figure S1). ExPaSy bioinformatics resource demonstrated protein translation of five different isoforms, and the amino acid sequences were deposited in NCBI database. *PmVago1* (GenBank: OQ730825) contained 498 bp and was translated into 165 amino acid residues with predicted 16.5 kDa MW and pI 4.67. *PmVago2* (GenBank: OQ730826) contained 318 bp for 105 amino acid residues (MW 11.3 kDa, pI 6.03), whereas *PmVago3* (GenBank: OQ730827) contained 318 bp for 105 amino acids (MW 11.12 kDa, pI 6.55). *PmVago4* (GenBank: OQ730828) harbored 408 bp encoding for 135 amino acids with 14.46 kDa and pI 4.6. *PmVago5* (GenBank: OQ730829) was 312 bp and translated into 103 amino acid residues with predicted MW of 10.99 kDa and pI 6.68 (Figure 1A). Protein domain analysis in SMART database predicted the conserved C-terminal single von Willebrand type-C domains (SVWC), which are involved in immune response stimulation. The SVW domains were located from amino acid residues 41 to 117 of *PmVago1*, 36 to 104 of *PmVago2*, 37 to 104 of *PmVago3*, 37 to 104 of *PmVago4*, and 36 to 102 of *PmVago5*. Moreover, *PmVago1* contained C-terminal KAZAL domain, N-terminal Zn-ribbon domain, and RIIa domain harboring phosphorylation site. *PmVago3* contained additional WAP domain from residues 32 to 65. The protease cleavage site was predicted only in *PmVago1* at amino acid residues 15 and 16 (Figure 1B).

Tissue distribution of *PmVago* transcripts in healthy *P. monodon*

PmVago1-5 transcripts were determined by semi-quantitative RT-PCR and expressed differently in examined tissues. *PmVago1*, *PmVago4*, and *PmVago5* exhibiting the specific bands at 326 bp, 362 bp, and 262 bp, respectively, showed the highest expression in the hemocytes, which is the immune-related tissue. Regarding *PmVago2* and *PmVago3*, the mRNA expression of the specific bands at 318 bp and 312 bp, respectively, was shown moderately in hemocytes. Meanwhile, *PmVago3* showed high preference for mRNA expression in hepatopancreas. The mRNA expression of elongation factor-1α gene (*EF1α*) with the specific band at 152 bp was used as an internal control (Figure 1C).

Multiple sequence alignment and phylogenetic analysis

The evolutionary relationship of *Pm*Vago1-5 and Vago-family proteins containing SVWC domain from other organisms was examined, including crustaceans, arthropods, and vertebrate. Sequence analysis using BLAST algorithm in NCBI database and Clustal2.1 demonstrated high similarity of Vago from *P. monodon* with *L. vannamei* (87.88%–99.68% identity) and *Marsupenaeus japonicus* (72.40%–97.22% identity). *Pm*Vagos exhibited moderate percent identity to *D. melanogaster* at 38.41%–46.36% (Figure S2A).

Multiple sequence alignment of amino acid residues in Clustal Omega revealed the important single von Willebrand domain, which is conserved among Vago and Vago-family proteins in the examined species. The protein motif features were predicted using SMART 8.0. As the result shown, the SVWC domain was highly conserved from *D. melanogaster* to among penaeid species including *P. monodon*, *L. vannamei*, and *M. japonicus*, until *Homo sapiens*. In addition, the conserved seven cysteine residues were indicated within SVWC domain except the last three residues in *Pm*Vago3, suggesting the possible unique structure in Vago-family proteins (Figure S2B).

The phylogenetic analysis was performed and exhibited the divided clusters comprising vertebrates and invertebrates. SVWC proteins from zebrafish (*Danio rerio*, NP_001268918.1), house mouse (*Mus musculus*, XP_006505981.1), and human (*H. sapiens*, AAB59458.1) were clustered in a group of vertebrates. Vago from fruit fly (*D. melanogaster*, NP_001285106.1) was clustered in the group of arthropods with crustaceans comprising *P. monodon*, *L. vannamei*, and *Penaeus* (*Marsupenaeus*) *japonicus*. Moreover, Vagos were divided namely according to their isoforms. The obvious groups of different Vago types were shown including Vago1 with SVC1, Vago2 with Vago3, Vago4 with SVC4, and Vago5 with SVC5. This result implied the unique conservation and evolutionary relationship of distinct Vago isoforms among different species (Figure 2).

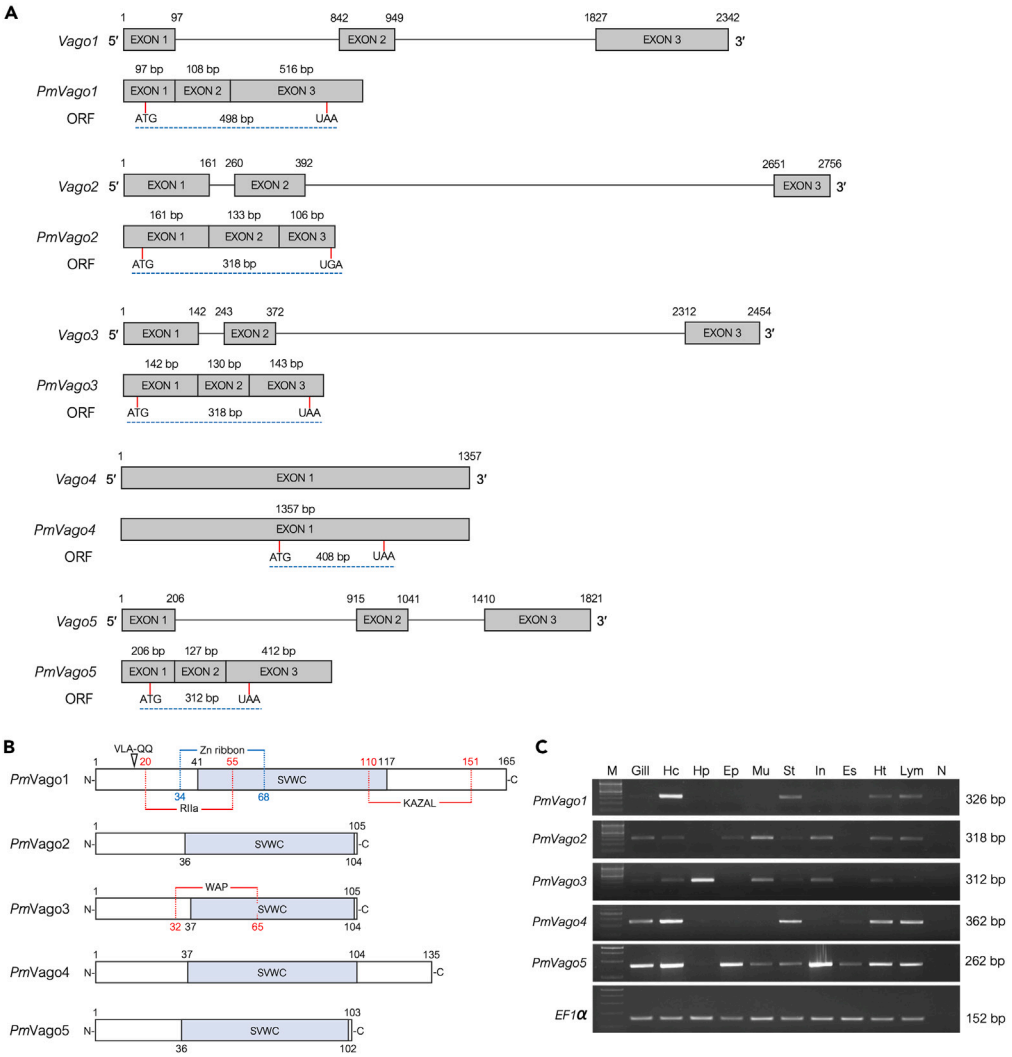

Figure 1. *Pm*Vago sequences retrieved from black tiger shrimp *Penaeus monodon* reference genome and tissue-specific mRNA expression

(A) Schematic diagrams of *Pm*Vago genomic organization structures and open reading frames including *PmVago1*, *PmVago2*, *PmVago3*, *PmVago4*, and *PmVago5*. Exons are depicted as boxes and introns as connecting solid lines. ORFs are depicted as blue dashed line. The numbers indicate sizes of exons and positions in genomic DNA sequences. Sequences are aligned in 5′–3′ direction. The start (ATG) and stop (UAA or UGA) codons are represented by red vertical bars.

(B) Schematic diagrams of *Pm*Vago domain topology. The amino acid sequences were deduced, and the important protein motif features were predicted. The conserved residues in single von Willebrand domain type-C (SVWC) are in blue boxes. The SVWC domains are located from amino acid residues 41 to 117 of *Pm*Vago1, 36 to 104 of *Pm*Vago2, 37 to 104 of *Pm*Vago3, 37 to 104 of *Pm*Vago4, and 36 to 102 of *Pm*Vago5. In addition, *Pm*Vago1 contains N-terminal Zn-ribbon domain and RIIa domain harboring phosphorylation site and C-terminal KAZAL domain, whereas *Pm*Vago3 contains additional WAP domain. The predicted cleavage site on amino acid residues 15 and 16 of *Pm*Vago1 is arrowed.

(C) Tissue distribution of *Pm*Vago1-5 transcripts in healthy *P. monodon* by semi-quantitative RT-PCR. Different tissues were collected for gene expression analysis including gill, hemocytes (Hc), hepatopancreas (Hp), epipodite (Ep), muscle (Mu), stomach (St), intestine (In), eyestalk (Es), heart, (Ht), and lymphoid organ (Lym). *Pm*Vago1, *Pm*Vago2, *Pm*Vago3, *Pm*Vago4, and *Pm*Vago5 transcripts exhibited the specific bands at 326 bp, 318 bp, 312 bp, 362 bp, and 262 bp, respectively. The expression of *Pm*EF1α (152 bp) was utilized as an internal control. N represented negative control.

Temporal expression profiles of *PmVago* mRNA after pathogen-induced immune challenges

The level of *PmVago* mRNA transcripts was determined following the infection by WSSV, YHV, and Vp_{AHPND}, using RT-qPCR at 0, 3, 6, 12, 24, and 48 h post-infection and EHP at 1, 7, 8, 9, 11, 13, 14, and 15 days post-cohabitation. WSSV highly stimulated *PmVago1* and *PmVago3* transcript levels at the early state of infection relatively to PBS control group and induced *PmVago5* lately. *PmVago2* was slightly decreased at 6h–12 h post-WSSV infection and gradually increased to the highest level at 48 h ($p < 0.05$). *PmVago4* was induced at 6 h post-WSSV early infection and highly induced at 48 h of late infection (Figure 3A). Meanwhile, an RNA virus YHV stimulated five isoforms of *PmVago* after infection. *PmVago1* and *PmVago4*

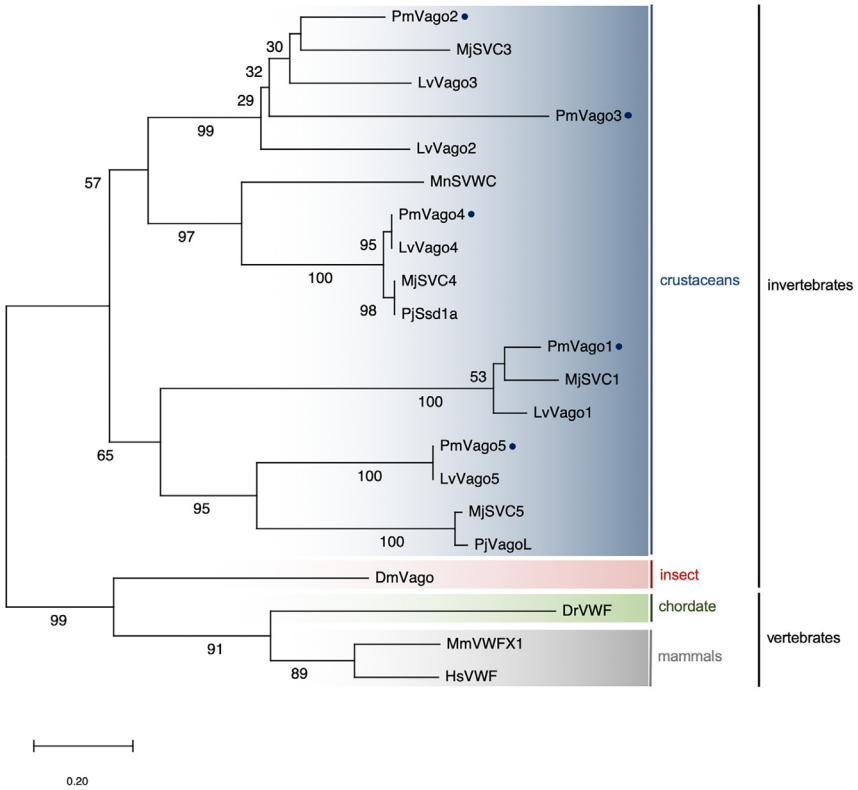

Figure 2. Phylogenetic analysis of Vago and Vago-family proteins from *P monodon* and various species

The neighbor joining (NJ) phylogenic tree was constructed in MEGA 7.0 software based on the amino acid sequences of *Pm*Vago1, *Pm*Vago2, *Pm*Vago3, *Pm*Vago4, *Pm*Vago5, and Vago-family proteins from vertebrates and invertebrates. Bootstrap sampling was reiterated for 1,000 times. The deduced amino acid sequences retrieved from various species include *P. monodon* Vago1 (*Pm*Vago1, WKV34892), *P. monodon* Vago2 (*Pm*Vago2, WKV34893), *P. monodon* Vago3 (*Pm*Vago3, WKV34894), *P. monodon* Vago4 (*Pm*Vago4, WKV34895), *P. monodon* Vago5 (*Pm*Vago5, WKV34896), *L. vannamei* SVWC1 (*Lv*Vago1, AEB54791.1), *L. vannamei* SVWC2 (*Lv*Vago2, AEB54792.1), *L. vannamei* SVWC3 (*Lv*Vago2, AEB54793.1), *L. vannamei* SVWC4 (*Lv*Vago4, XP_027223835.1), *L. vannamei* SVWC5 (*Lv*Vago5, AEB54795.1), *M. japonicus* SVC1 (*Mj*SVC1, LC075213.1), *M. japonicus* SVC3 (*Mj*SVC3, LC114987.1), *M. japonicus* SVC4 (*Mj*SVC4, LC075214.1), *M. japonicus* SVC5 (*Mj*SVC5, LC075215.1), *M. nipponense* SVWC (*Mn*SVWC, MK125517.1), *P. japonicus* Vago-L (*Pj*VagoL, OK169909.1), *P. japonicus* Ssd1a (*Pj*Ssd1a, XM_043036179.1), *D. melanogaster* Vago (*Dm*Vago, NP_001285106.1), *H. sapiens* VWF (*Hs*VWF, AAB59458.1), *D. rerio* VWF (*Dr*VWF, NP_001268918.1), and *M. musculus* VWFX1 (*Mm*VWFX1, XP_006505981.1).

reached the highest stimulation after YHV infection at 6 h and gradually decreased until 24 h post-infection. At 12 h, the highest expression of *Pm*Vago2 and *Pm*Vago5 was detected, whereas that of *Pm*Vago3 was evidenced at 48 h ($p < 0.05$) (Figure 3B).

Following a bacterial infection from Vp_{AHPND}, *PmVago1* transcript was mainly increased after 3 h, whereas a high expression of *PmVago2* and *PmVago3* was clearly observed at 48 h of late infection. The infection from Vp_{AHPND} notably induced *PmVago4* and *PmVago5* at 24 h (Figure 3C).

Infection from EHP demonstrated varied expression patterns of *PmVago* isoforms. *PmVago1* was induced and showed statistical difference on days 9 and 11 similar to *PmVago2* on days 7, 11, and 13. Meanwhile, *PmVago3* exhibited no significant difference following EHP infection. *Vago4* was decreased on day 9 until day 11 and increased significantly on days 14 and 15. *Pm*Vago5 was temporarily decreased on day 9 and showed statistically highest induction on day 11 before its downregulation from days 13–15 (Figure 3D).

The results indicated significant mRNA expression levels of *PmVago1-5* normalized to *PmEF1α* transcript level and compared to the control group ($p < 0.05$). Since *PmVago1*, *PmVago4*, and *PmVago5* highly responded against WSSV that is the most severe viral pathogen in shrimp farming, they were further functionally investigated upon WSSV infection.

Efficiency of *in vivo* dsRNA-mediated *PmVago* RNA interference and its effects on shrimp cumulative mortality upon WSSV infection and virus replication

To investigate the crucial roles of *PmVago1*, *PmVago4*, and *PmVago5* in shrimp immune response, dsRNA-mediated RNA interference was performed. Quantitative RT-PCR was carried out to show the significant suppression on *PmVago1*, *PmVago4*, and *PmVago5* transcripts following dsRNA injection (5 μg/g shrimp body weight). The expression of *PmVago1* was significantly decreased to 0.2-fold at 24 h and 0.44-fold at 240 h, whereas, *PmVago4* was expressed by 0.03-fold at 24 h and 0.29-fold at 240 h following their specific RNAi separately

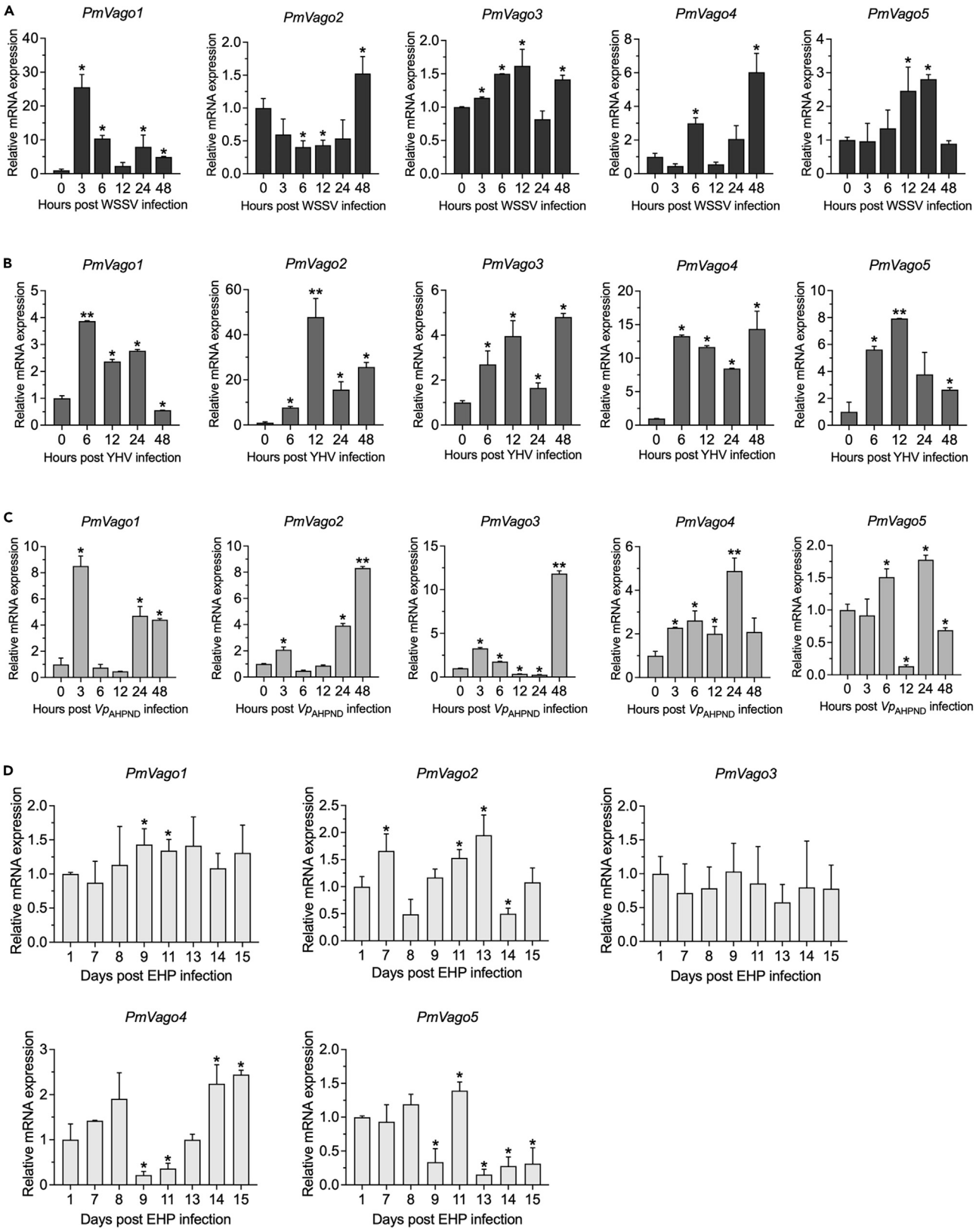
A
PmVago1
PmVago2
PmVago3
PmVago4
PmVago5
Relative mRNA expression
Hours post WSSV infection
B
PmVago1
PmVago2
PmVago3
PmVago4
PmVago5
Relative mRNA expression
Hours post YHV infection
C
PmVago1
PmVago2
PmVago3
PmVago4
PmVago5
Relative mRNA expression
Hours post Vp_{AHPND} infection
D
PmVago1
PmVago2
PmVago3
PmVago4
PmVago5
Relative mRNA expression
Days post EHP infection

Figure 3. Temporal gene expression profiles of *PmVago1, PmVago2, PmVago3, PmVago4,* and *PmVago5* in *P monodon* after immune challenge with infectious pathogens

Shrimp were randomly collected after infection with (A) White spot syndrome virus, (B) Yellow head virus, (C) *Vibro parahaemolyticus* AHPND, and (D) *Enterocytozoon hepatopenaei* at the indicated time points. *PmVago* transcript expression in hemocyte was determined by RT-qPCR. The relative mRNA expression was calculated according to Pfaffl method (2001) using *PmEF1α* as a reference gene compared to PBS-injected control group. The experiments were performed in three independent triplicates of three shrimp and shown as the means ± SDs. Asterisks indicate significant differences of mean values ($p < 0.05$).

compared to the dsGFP control groups. ($p < 0.05$). In addition, *PmVago1* was induced approximately to 1.52- to 1.97-folds after *PmVago4* suppression, and similarly, *PmVago4* increased to 2.63- to 3.26-folds after *PmVago1* suppression (Figure 4A). Moreover, there was no significant non-specific suppression from dsPmVago1 and dsPmVago4 on *PmVago2*, *PmVago3*, and *PmVago5* transcript levels after dsRNA injection ($p < 0.05$) (Figure 4B).

To examine the effect of *PmVago1*, *PmVago4*, and *PmVago5* RNAi upon WSSV infection, shrimp were injected with either dsPmVago1+dsPmVago4 or dsPmVago5 prior to WSSV infection, and the cumulative mortalities were recorded compared to the control. With dsRNA cocktail (dsPmVago1+dsPmVago4), *PmVago1* and *PmVago4* were suppressed simultaneously to reduce the compensatory effect from either isoform. The mRNA expression of *PmVago1*, *PmVago4*, and *PmVago5* was successfully reduced (Figure S4). Suppression of *PmVago* resulted in a higher susceptibility to rapid death compared to dsGFP-injected shrimp. Following WSSV infection, the dsPmVago1+dsPmVago4 and dsPmVago5 groups demonstrated a 100% mortality on days 6 and 9, respectively. Meanwhile, the dsGFP group showed 100% mortality on day 10. The suppression of *PmVago1+PmVago4* exhibited 50% cumulative mortalities after 3 days, whereas that of *PmVago5* was shown after 5 days (Figure 4C). The high mortality rates suggested the significant roles of *PmVago1* and *PmVago4* for shrimp survival upon WSSV infection.

The consequence effect of *PmVago1*, *PmVago4*, and *PmVago5* suppression on WSSV replication was further investigated. The conserved *VP28* genes representing WSSV genome copies were absolutely quantitated against *VP28* internal standard until day 5, which covered the time points that exhibited 50% cumulative mortalities. As shown in Figure 4D, WSSV replication significantly increased in *PmVago1+PmVago4*-and *PmVago5*-suppressed shrimp compared to dsGFP group ($p < 0.05$). The viral copy number detected was increased correlated with the cumulative mortalities shown. However, the high mortality rate and WSSV replication in dsPmVago1, dsPmVago4 (Figure S5), and dsPmVago1+dsPmVago4 shrimp suggested the significant roles of *PmVago1* and *PmVago4* for shrimp survival upon WSSV infection over *PmVago5*.

Effects of *PmVago1* and *PmVago4* RNA interference on immune-related genes upon WSSV infection

To examine the RNAi effects of the high WSSV-responding *PmVago* isoforms on immune-related genes, shrimp were injected with either dsPmVago1+dsPmVago4 or dsGFP. The suppressed shrimp were subsequently infected with WSSV or PBS as the control. The transcript levels of AMPs, immune receptors, and signal transducers were determined. Compared to the dsGFP control group, the important signal mediators such as *Cactus*, *Relish*, *Dorsal*, and *IKKε1* were decreased besides genes in JAK/STAT pathway (*Domeless*, *JAK*, *STAT*) and a cytokine-like *Spätzle* following *PmVago1+PmVago4* suppression (Figure 5A). Similarly, the AMP genes were significantly reduced after *PmVago1+PmVago4* suppression ($p < 0.05$) (Figure 5B), whereas *CrustinPm1* and *Penaeidin*5 were not affected by separated RNAi of dsPmVago1 or dsPmVago4 (Figure S6). Interestingly, *CrustinPm7* was significantly upregulated by *PmVago4* suppression. In addition, the transcript level of *IMD* remained statistically unaffected compared to dsGFP control ($p < 0.05$).

*Pm*Vago1 and *Pm*Vago4 RNAi resulted in lowered proPO gene transcripts and hemolymph phenoloxidase activity

The *in vivo* suppression of *PmVago1* and *PmVago4* further demonstrated the subsequence on immune genes involved in proPO system. Following *Vago* suppression, *PmproPO1*, *PmproPO2*, *PmPPAE1*, and *PmPPAE2* transcripts showed significant decrease compared to the control dsGFP group (Figure 6A). To examine the consequence of *PmVago* suppression on shrimp proPO system, PO activity in shrimp hemolymph was performed *in vitro*. As the results, a significant reduction of the PO activity to 31.25% compared to the control dsGFP was observed in the dsPmVago1-injected group, whereas dsPmVago4 resulted in 23.12% of the remaining PO activity ($p < 0.05$). The results of basal PO activity in normal dsGFP shrimp was utilized as an internal control for significant difference in PO activity (Figure 6B). Thus, *PmVago1* and *PmVago4* possibly function as the stimuli of shrimp proPO system.

Cellular localization of *Pm*Vago1 and *Pm*Vago4 in hemocytes of healthy and WSSV-infected *P. monodon*

To monitor the cellular localization of Vago against WSSV infection, the most WSSV responding isoforms including *Pm*Vago1 and *Pm*Vago4 were selected. As shown in the microscopic Figure 7A, *Pm*Vago1 and *Pm*Vago4 were detected in all three types of hemocytes (hyaline cells, HC; granular cells, GC; semi-granular cells, SC). *Pm*Vago1 was localized in both nucleus and cytoplasm, whereas *Pm*Vago4 was mainly distributed in nucleus and only slightly detected in the cytoplasm. Interestingly, the obvious signals were detected after WSSV infection for 24 h, indicating the translocation of *Pm*Vago1 and *Pm*Vago4 to cytoplasm. *Pm*Vago4 was found partially located in granules of granulocyte cells (GC) (Figure 7B). At 48 h, the signals of *Pm*Vago1 and *Pm*Vago4 were reduced in cytoplasm (Figure 7C). In contrast, the high signals from *Pm*Vago1 and *Pm*Vago4 were observed in cell membrane with high WSSV loads (Figure 7D). Western blot analysis was performed and confirmed the reduction in protein amount of *Pm*Vago1 and *Pm*Vago4 contained in hemocyte after WSSV infection (Figure 7E) in addition to the reduced localization in nucleus (Figure 7F).

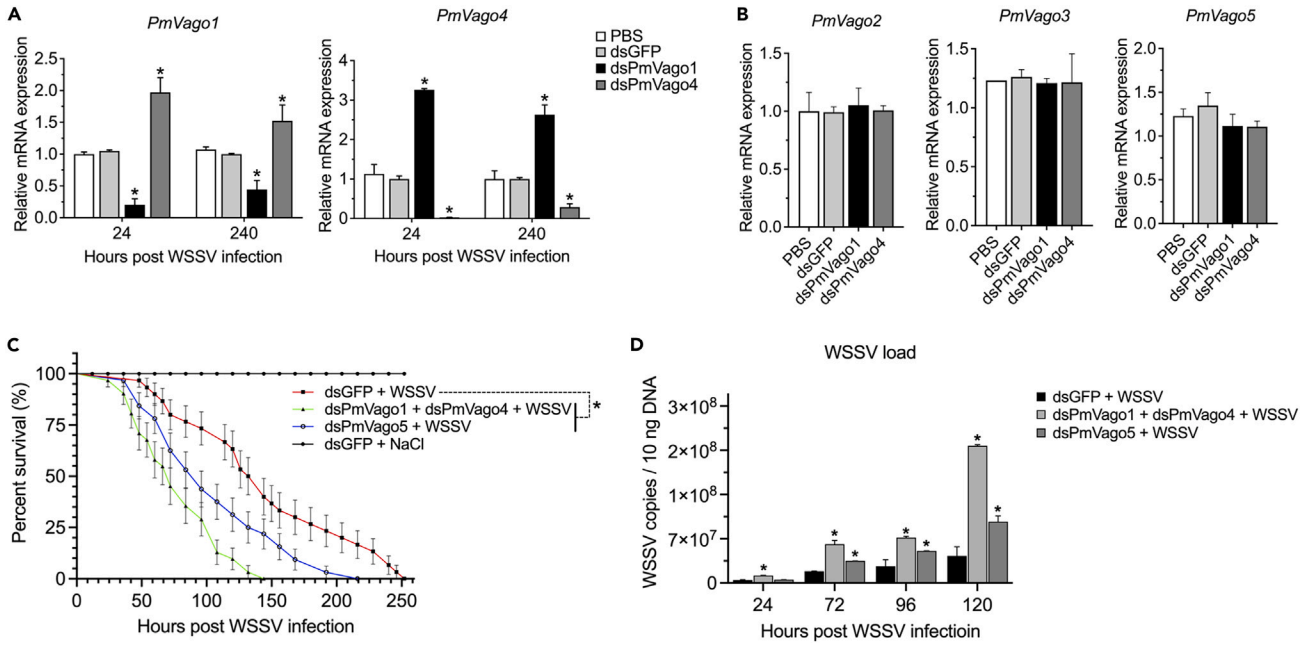

Figure 4. Effects of *PmVago1*, *PmVago4*, and *PmVago5* suppression on WSSV copy number and shrimp survival

(A) Expression profiles of *PmVago1* and *PmVago4* after specific dsRNA-mediated RNAi. Suppression of *PmVago1* and *PmVago4* resulted in the expression compensation between the two isoforms.

(B) *PmVago1* and *PmVago4* were specifically suppressed without cross reactivity of dsRNA on different isoforms.

(C) Percent survival (%) of *PmVago1*+*PmVago4*-and *PmVago5*-suppressed shrimp after WSSV infection. The experiments were performed in triplicates, and the cumulative mortalities were recorded daily for 10 days. The experiment was performed in three independent triplicates of 30 shrimp per group.

(D) WSSV numbers in gill tissues of *PmVago1*+*PmVago4*- and *PmVago5*-suppressed shrimp post-WSSV infection. The WSSV number was quantified using genomic DNA from gill at selected time points by RT-qPCR analysis. The column represents the median of the results (means ± SDs with $n = 3$). The data were analyzed statistically by one-way ANOVA (*$p < 0.01$) and shown as the means ± SDs with $n = 3$.

*Pm*Vago1 and *Pm*Vago4 overexpression promoted Dorsal and Relish transcription activity regarding to IKK-mediated stimulation in HEK293T cells

To evaluate the regulation of *PmVago* under the IKK-NF-κB signaling pathway *in vivo*, dual luciferase assay was performed. Since *PmVago1* and *PmVago4* were mainly involved in WSSV response and affected by IKK suppression (Figure S7), they were further investigated under IKK-NF-κB regulation. The core promoter regions of *PmVago1* and *PmVago4* were identified and cloned into pGL3-basic reporter plasmid with predicted transcription factor binding sites (Figure 8A). HEK293T cells were divided and transiently cotransfected with pcDNA3-*PmIKK*-Myc expression plasmid and pGL3-*PmVago* luciferase reporters constructs in Figure 8B. After 24 h, cells were harvested for protein detection and luciferase activity. The recombinant proteins including *Pm*IKKβ, *Pm*IKKε1, *Pm*IKKε2, *Pm*Vago1, and *Pm*Vaog4 were expressed in HEK293T cells (Figure 8C). Compared to the control, *PmVago1* promoter was approximately induced by 6.06-, 27.45-, and 11.03-fold by *Pm*IKKβ, *Pm*IKKε1, and *Pm*IKKε2 overexpression, respectively. In addition, luciferase activity driven by *PmVago4* promoter was significantly induced to 2.88-, 1.49-, and 2.16-fold by *Pm*IKKβ, *Pm*IKKε1, and *Pm*IKKε2 ($p < 0.01$) (Figure 8D).

To further determine the stimulation activity of *Pm*Vago1 and *Pm*Vago4 against the other immune cascade, Dorsal and Relish were selected as the important mediators in shrimp immune pathways. As the results, *Dorsal* promoter was stimulated to 6.8-fold by *PmVago1* and 6.37-fold by *PmVago4* compared to the control group. Besides, *Relish* promoter showed the elevated luciferase activity by 5.24- and 5.82-fold ($p < 0.01$) as the results of *PmVago1* and *PmVago4* overexpression, respectively (Figure 8D). The results demonstrated the possible regulation of *Pm*Vago1 and *Pm*Vago4 under IKK-NF-κB cascade and, in turn, could act to further stimulate signaling cascades involving Dorsal and Relish as proposed in Figure 9.

DISCUSSION

The cytokine system consists of signaling molecules that regulate the immune system and maintain cellular network homeostasis. In vertebrates, cytokines are small peptides and types of biomolecules produced by various cells as the messengers between the complex signaling cascades such as JAK/STAT, Toll, IMD, and IKK-NF-κB pathways.[2,10] Although less cytokine mechanisms have been reported in crustacean innate immune system, recent study exhibited the possible regulation of the cytokine-like Vago in IKK-NF-κB signaling pathway of Penaeid

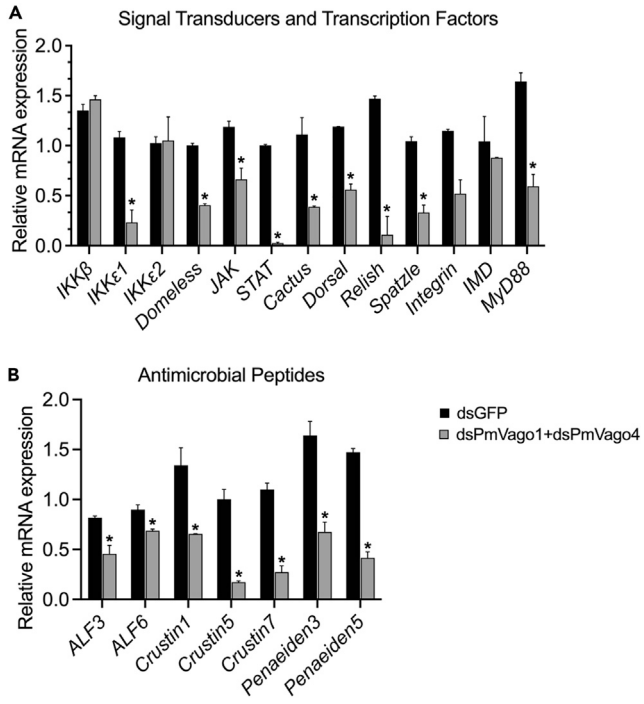

Figure 5. Subsequent effects of *PmVago1* and *PmVago4* suppression by dsRNA-mediated RNAi on immune-related genes following WSSV infection

The transcript levels of the important immune-related genes were determined by RT-qPCR.

(A) Expression profiles of immune receptors and signal transducers were determined following *PmVago1+PmVago4* suppression compared to the dsGFP control group. The important genes were involved in signal cascades such as IKK-NF-κB, Toll, IMD, and JAK/STAT pathways.

(B) Groups of the major antimicrobial peptide genes involved in shrimp innate immune response were monitored following *PmVago1+PmVago4* suppression. The data shown were normalized with *EF1α* as the reference gene and represented as the mean fold change (means ± SDs, n = 3) relatively to the control group. The statistical difference was analyzed at $*p < 0.05$.

shrimp and *D. melanogaster*.[3,16,21] In this study, the *Vago* from black tiger shrimp *Penaeus monodon* (*PmVago*) were identified and characterized for their possible cytokine-like function in the correlation with IKK-NF-κB pathways.

Five isoforms of *Vago* from *P. monodon* were successfully identified, designated *PmVago1-PmVago5* based on our *P. monodon* EST database and the data previously released from other Penaeid species and arthropods. The phylogenetic analysis revealed the evolutionary clusters of *PmVago* that was closely related to *Vago* from L. *vannamei* and *M. japonicus* with lower developmental connection to Vago-family proteins of vertebrates. According to protein feature analysis, Vago from *P. monodon* harbored the single von Willebrand domain (SVWD) as shown in *Lv*Vago and *Mj*Vago. The SVWD was conserved and shared approximately 87%–94% of high similarities at the protein level from arthropods to vertebrates.[22,23] The domain was recognized by the interferon regulatory factor (IRF) and evidenced in *Lv*IRF-Vago pathway activation for WSSV response through *LvTRAF3*.[3] Protein analysis of *Mj*Vago L-type (*Mj*Vago-L) showed the VWD type-C (VWC), which was similar to the crucial cysteine-rich-proinflammatory responding protein (CCN3) in mammal.[24] Comparable to *Drosophila*, the *Dm*Vago polypeptide contained a SVWC with 8–10 conserved cysteine residues found only in arthropods as also shown in its orthologue from *Culex* mosquito (*Cx*Vago).[18,25] This accumulating sequence analysis data demonstrated the homologous identity between *Vago* identified in arthropods and crustaceans with von Willebrand factor protein (VWF) from vertebrates.[23,26] In human and murine, VWF regulated primary hemostasis and directed the effects upon proinflammatory responses. VWF binding to receptors initiated intracellular downstream signaling including phosphorylation of the MAPKinase p38 and JNK in addition to NF-κB activation, leading to the secretion of proinflammatory cytokines and chemokines.[27] Besides, the SVWDs in *Macrobrachium nipponense* has been proposed to elicit antiviral activities as an interferon analog.[23] Therefore, the SVWD composition of *PmVago* was relatable as the primary hallmark of their biological functions in immune-related signaling cascade.

From the tissue-specific expression in healthy *P. monodon* and temporal expression of *Pm*Vago transcripts upon WSSV infection, *PmVago1*, *PmVago4*, and *PmVaog5* were selected for further functional characterization. The particular high transcript levels of *PmVago1*, *PmVaog4*, and *PmVaog5* were observed in the hemocytes (Hc), which were wildly recognized as the cellular arm in innate immune response.[9,28] They encapsulated parasites and other foreign bodies, mediating melanization reaction and secretion of JAK/STAT-activating cytokines. Quantitative PCR analysis demonstrated that *PmVago1*, *PmVaog4*, and *PmVaog5* transcripts were mainly upregulated upon WSSV infections, whereas the rest isoforms were moderately stimulated. Similarly, *AeVago1* in *Aedes aegypti* mosquito was induced by dengue virus and contributed to limiting virus replication.[29] This was consistent with *Culex* mosquito during West Nile virus (WNV) infection, the

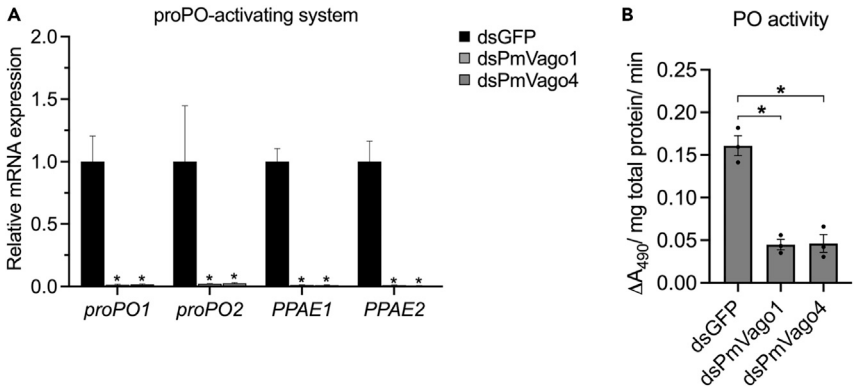

Figure 6. Effects of *Pm*Vago1 and *Pm*Vago4 RNAi on proPO-associated genes and PO activity upon WSSV infection

(A) The effect of *Pm*Vago1 and *Pm*Vago4 suppression on the mRNA transcripts of genes involved in the proPO system (*Pm*proPO1, *Pm*proPO2, *Pm*PPAE1, and *Pm*PPAE2). Gene transcription level was evaluated by RT-qPCR using specific primers for each gene at 24 h (Table S1). Data were normalized relatively to a reference gene *EF1-α* and shown as the mean fold change (means ± SDs, n = 3). The average relative expressions are representatives of three independent replicates. Significant difference compared with control is indicated by an *asterisk* ($p < 0.01$).

(B) Reduction of PO activity following *Pm*Vago1 and *Pm*Vago4 RNAi. The proPO activation from shrimp hemocyte lysate was measured after preincubation *in vitro* with LPS. PO activity was defined as ΔA_{490}/mg of total protein/incubation minutes. The data are shown as the mean ± SDs and are derived from three independent replicate experiments. Statistical difference was calculated with $*p < 0.05$.

*Cx*Vago was induced as a cytokine stimulating a cell-specific antiviral response. *Cx*Vago acted as the interferon homolog activating the immune response and limiting virus replication in neighboring cells.[18,25] The *Dm*Vago was also reported as a virus-stimulated molecule that subsequently triggered an infected-state of the neighboring cells.[30,31] For *P. monodon*, the different *Vago* isoforms may participate in the various pathways of the response. To depict, *Vago5* in *P. vannamei* responded to Vp_{AHPND} infection through the NF-κB modulation and JAK/STAT pathways,[17] whereas *LvVago4* was highly responsible to the IRF compared to *LvVago5* under virus infection.[3] *MjVago*L was further identified as a possible ligand for a cytokine-induced integrin receptor in addition to the JAK/STAT pathway.[24] However, the pathways regulating the different Vago isoforms require further verification. For crustacean species, WSSV is one of the most lethal viral pathogens. *PmVago1* and *PmVago4* suppression exhibited high susceptibility during WSSV infection over *PmVago5*. The high WSSV copy number was detected as the shrimp cumulative mortality was elevated. The result indicated the Vago essential role in shrimp antiviral response and survival against WSSV replication.

Following WSSV infection, *Pm*Vago4 was released into cytoplasm and accumulated in the hemocyte granules and later reduced significantly as the virus increased, whereas *Pm*Vago1 was moderately detected in nucleus and cytoplasm. Moreover, *Pm*Vago4 was found accumulated around the area of cell membrane. The results implied the possible cytokine-like mechanism of Vago storage and secretion upon WSSV infection as reported in *Culex* previously. The *Cx*Vago protein was increased during WNV infection in a time-dependent manner and secreted to activate the JAK/STAT pathway.[18] In *L. vannamei*, Vago was reported as it might function as an IFN-like molecule and shrimp possibly possess an antiviral mechanism similar to the IFN system.[3] Moreover, the Drosophila C virus (DCV) infection experiments have identified that the JAK-STAT receptor *Dm*Domeless was an orthologue of mammalian class I cytokine receptors,[32] yet, the specific immune receptor for *Pm*Vago needs to be identified.

In addition, *PmVago1* and *PmVago4* affected the transcription of several immune-related genes including inhibitor of kappa B kinases (*PmIKK*). In reverse, *PmVago4* was previously found regulated by *PmIKKβ* and *PmIKKε*.[16] The additional result further confirmed the correlation of *PmVago1* and *PmVago4* regulation by *PmIKK* expression (Figure S7). Our previous study demonstrated that expression of *PmVago1* and *PmVago4* but no other isoforms was mainly reduced following IRF mRNA suppression,[33] suggesting that IRF might mediate the pathway regulating *PmVago1* and *PmVago4* expression. Additional IKK genes knockdown experiment showed a strong reduction of IRF (Figure S3) and Vago suppression (Figure S7), implying that IKK-IRF also mediated *PmVago1* and *PmVago4* expression. Thus, our study reported the additional information of Vago regulation via IKK-NF-κB cascade as a possible alternative pathway to the IRF as proposed in Figure 9. In fruit fly, *DmIKK* modulated the host immune response through *Dm*IFNβ and IRF stimulation.[34] In innate immune system, IKKβ and IKKε were the upstream regulators of the IKK-NF-κB signaling to activate cytokines.[12,15,34] In this study, the *PmIKKβ* upregulation after *PmVago* suppression was possibly the effect of pro-inflammatory stimulation. As shown in mammals, IKKβ compensated for the lack of IKKα to modulate the NF-κB factors,[35,36] which was either independent to the IKKε activity.[37] These data primarily evidenced the distinct roles of *Pm*Vago on the different IKKβ and IKKε isoforms in shrimp alternative immune pathways. In *D. melanogaster* and Penaeid shrimp, the IKK-NF-κB pathway promoted the production of the canonical antimicrobial peptides (AMPs).[12,14]

In this study, *PmPenaeidin*, *ALFPm*, and *PmCrustin* were significantly reduced along with signal transducers (*PmDorsal*, *PmCactus*, *PmMyD88*, and *PmRelish*) upon *PmVago1* and *PmVago4* suppression. The results demonstrated the significant connection of *Pm*Vago to Toll and IMD pathways. As shown previously, *ALFPm3* and *crustinPm7* were involved in both Toll and IMD pathways,[38,39] whereas *ALFPm6* and *crustinPm*1 were under Toll pathway.[40] Further study in *Fraxinus chinensis* with WSSV and *Vibio anguillarum* infection revealed the

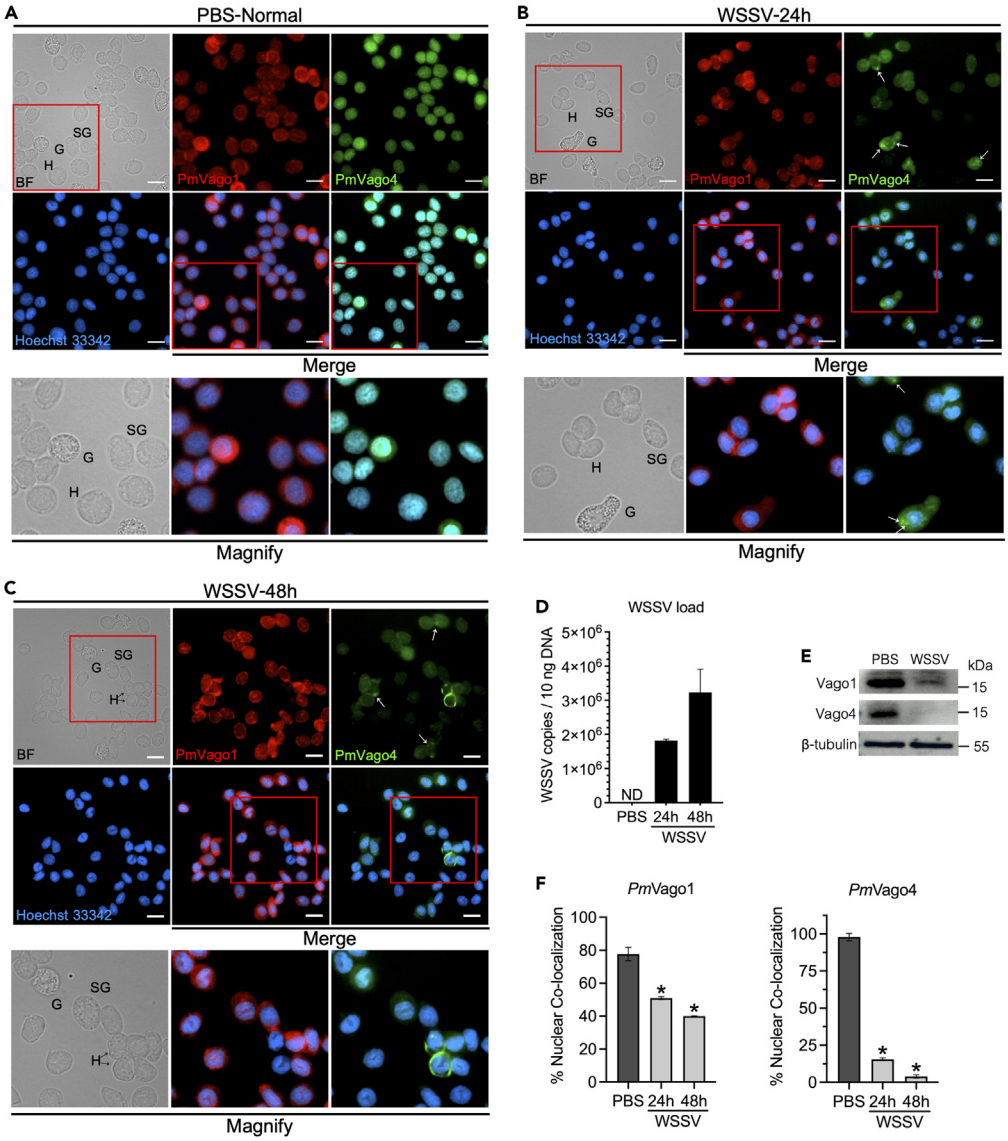

Figure 7. Cellular localization of *Pm*Vago1 and *Pm*Vago4 in *P monodon* hemocytes upon WSSV infection

*Pm*Vago1 and *Pm*Vago4, the most WSSV responding isoforms, were detected for cellular localization in response to WSSV infection. Shrimp were divided and infected with WSSV inoculum or PBS for control. Total hemocytes were collected from three random shrimp at 24 h and 48 h post-infection and fixed immediately with 4% (w/v) paraformaldehyde in 1X PBS for immunofluorescence staining. *Pm*Vago1 was labeled red with goat anti-rabbit antibody conjugated with Alexa Fluor568 (Thermo Scientific), whereas *Pm*Vago4 was labeled green with rabbit anti-mouse antibody conjugated with Alexa Fluor488 (Thermo Scientific). Nuclei were stained blue with Hoechst 33342 (Thermo Scientific). Cells were observed under LSM700 laser scanning confocal microscope (Carl Zeiss) in bright field (BF) and dark field. All three types of hemocytes were identified including hyaline cells (HC), granular cells (GC), and semi-granular cells (SGC).

(A) Cellular localization of *Pm*Vago1 and *Pm*Vago4 under PBS non-infection condition.

(B) and (C) Cellular translocation of *Pm*Vago1 and *Pm*Vago4 following WSSV infection after 24 and 48 h, respectively.

(D) Viral load was not detected in PBS-shrimp and WSSV replication folds in infected group after indicated time points.

(E) Immunoblotting exhibited the reduction of endogenous *Pm*Vago1 and *Pm*Vago4 in hemocytes upon WSSV infection. β-tubulin was detected as an internal control.

(F) Nuclear colocalization percentage of *Pm*Vago1 and *Pm*Vago4 post-WSSV infection correlated to Hoechst33342-stained areas calculated by WCIF ImageJ software.The data was shown as means and SD from three independent replicates statistically analyzed with $*p < 0.05$.

decrease of *FcPenaeidin* following *FcDorsal* suppression under Toll pathway.[41,42] The IMD pathway was mediated by *Relish* and involved with *PmPEN3* and *PmPEN5*.[40,42] This *PmVago1* and *PmVago4* suppression suggested the contribution of *Pm*Vago to the different alternative downstream responses. The regulation of *Pm*Vago in *P. monodon* IKK-NF-κB cascade was further demonstrated by luciferase reporter. *Pm*IKKε1 highly activated *PmVago1*, whereas *Pm*IKKβ and *Pm*IKKε2 show positivity on *PmVago4*. Following IKK activation, *Pm*Vago1 and

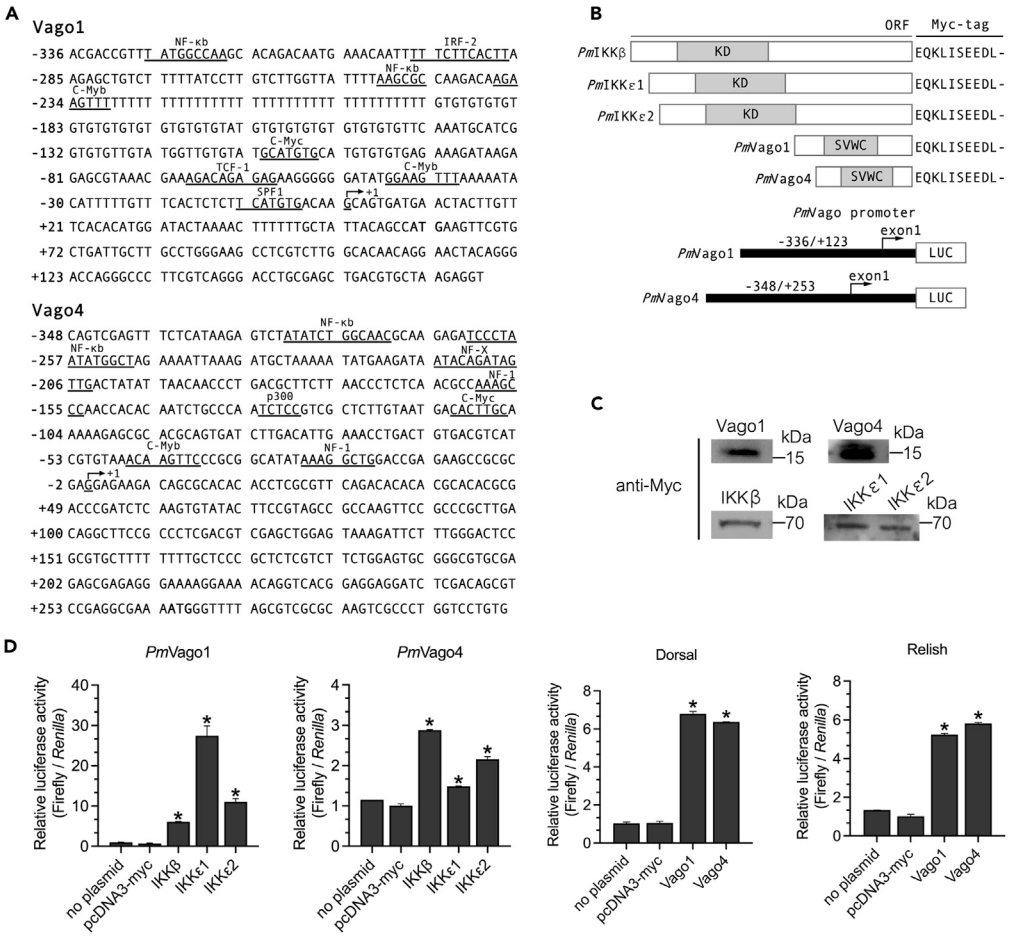

Figure 8. Promoter regulation of *PmVago* activated by inhibitor of kappa B kinases (IKK) overexpression promoted *PmDorsal* and *PmRelish* transcription activities in HEK293T cells

Cells were transiently cotransfected with luciferase reporter plasmids, a construct of protein expression plasmids as indicated along with *Renilla* luciferase plasmid as an internal control. The control groups were transfected with pcDNA3-Myc empty vector or grown without plasmid.

(A) The core promoter regions of *PmVago1* (−336 to +123) and *PmVago4* (−348 to +253) were identified with different types of transcription factor binding sites predicted by ALGGEN-PROMO search (underlined regions). The arrow denoted the transcription start sites, and the start codon (ATG) is shown in bold font.

(B) The constructs for protein expression plasmids with Myc-tag and *Vago* promoter reporters used for this study. The ORFs of *PmIKK* with important kinase domain (KD) and *PmVago* were cloned into pcDNA3.1-c-Myc for protein expression. The promoter regions of *PmVago* were cloned into pGL3-basic for luciferase reporters.

(C) *In vivo* recombinant protein expression was confirmed in HEK293T cells with western blot analysis and anti-Myc antibody.

(D) The effects of *Pm*IKKβ and *Pm*IKKε overexpression on relative luciferase activity of *PmVago1* and *PmVago4* promoters and effects of *Pm*Vago1 and *Pm*Vago4 overexpression on *PmDorsal* and *PmRelish* promoter activities. Luciferase activities from reporter plasmids were determined at 24 h post-transfection and normalized on the basis of *Renilla* luciferase activity with Dual-Luciferase Reporter Assay System (Promega). Data are shown as the means ± SDs of normalized luciferase activities from triplicate experiments (n = 3). Asterisks indicate significant differences of mean values calculated by one-way ANOVA (*$p < 0.01$).

*Pm*Vago4 potentially stimulated the *PmDorsal* and *PmRelish* promoters, which are the two particular NF-κB transcription factor homologs.[34,42] These results demonstrated the activation of *Pm*Vago as the cytokine-like molecule by the Dorsal and Relish homologs in IKK-NF-κB signaling cascade. In addition, the important receptors Toll, IMD, and Domeless in JAK/STAT pathway and proPO-activating system were affected by *Vago* suppression. These cascade components activated AMP reporters and NF-κB in the promoter regions.[41,42] *PmVago* was linked to proPO-activating system producing the reactive melanin intermediates for a rapid pathogen response.[43,44] *PmVago1* and *PmVago4* suppression reduced *proPO1*, *proPO2*, *PPAE1*, and *PPAE2* transcripts, which subsequently affected the PO activity. These results depicted the IKK-NF-κB-Vago axis of modulation that provide the cross-talking between related immune pathways.

To summarize, from the distinct five *PmVago* isoforms identified in *P. monodon*, *PmVago1* and *PmVago4* were the two isoforms that highly connected to immune response to WSSV through AMPs, proPO-activating system, and immune-related genes. They exhibited as the possible cytokine-like molecules by cellular translocation under WSSV infection. The mechanism of *PmVago1* and *PmVago4* was initially

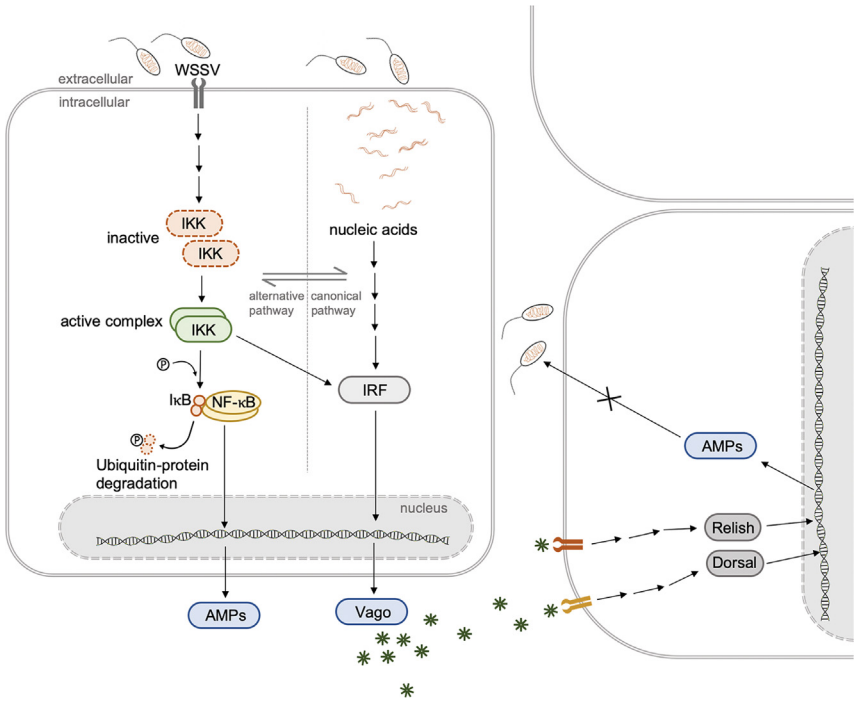

Figure 9. Proposed model mechanism of this study for Vago regulation via IKK-NF-κB cascade as a possible alternative pathway to the IRF

WSSV induced the expression and release of Vago through activation of IKK-Vago in the cytokine-like system. The released Vago further activated the immune cascade in the neighboring cells involving Dorsal and Relish, leading to AMP expression.

investigated under the IKK-NF-κB cascade in addition to the wildly reported canonical JAK/STAT pathway. They further stimulated the immune cascades by activating the important transcription factors *PmRelish* and *PmDorsal*. Collectively, these data underlined the potential roles of *Pm*Vago under the IKK-NF-κB cascade against WSSV infection in *P. monodon*, and the further cytokine-like regulation mechanism is an issue for further investigation.

Limitations of study

The study depicted the correlation of IKK-NF-κB signaling cascade and Vago modulation besides the canonical regulation under JAK/STAT pathway in *Penaeus monodon* innate immune system. However, the in-depth mechanism of Vago in cytokine-like system mediating innate immune response is elusive.

STAR★METHODS

Detailed methods are provided in the online version of this paper and include the following:

- KEY RESOURCES TABLE
- RESOURCE AVAILABILITY
  - Lead contact
  - Materials availability
  - Data and code availability
- EXPERIMENTAL MODEL AND STUDY PARTICIPANT DETAILS
  - Experimental shrimp and ethics statement
  - Preparation of shrimp pathogens
- METHOD DETAILS
  - Nucleotide cloning and sequencing of *Vago* from *P. monodon*
  - Bioinformatics analysis
  - Tissue distribution analysis of *PmVago*
  - Expression profiles of *PmVago1-5* in responses to viral, bacterial, and microsporidian challenges
  - Double-stranded RNA synthesis and *in vivo* suppression efficiency by dsRNA-Mediated RNA interference (RNAi)
  - Survival rates of *PmVago*-suppressed shrimp after WSSV infection

- Quantification of WSSV copy number in *PmVago*-Suppressed shrimp
- *PmVago* suppression effects on immune-related genes after WSSV infection
- Prophenoloxidase activity assay in *PmVago1*-and *PmVago4*-suppressed shrimp
- Immunofluorescence microscopic detection of *Pm*Vago1 and *Pm*Vago4 in shrimp hemocytes
- Immunodetection of *Pm*Vago protein in hemocytes
- Cell culture and plasmid construction
- Dual luciferase reporter assay

● QUANTIFICATION AND STATISTICAL ANALYSIS

SUPPLEMENTAL INFORMATION

Supplemental information can be found online at https://doi.org/10.1016/j.isci.2024.110161.

ACKNOWLEDGMENTS

This research project was supported by The Second Century Fund (C2F), Chulalongkorn University, to Z.N. and Thailand Science Research and Innovation Fund, Chulalongkorn University to A.T. In addition, the project was funded by The 90th Anniversary of Chulalongkorn University Fund (Ratchadaphiseksomphot Endowment Fund), Chulalongkorn University (Grant No. GCUGR1125652045D No. 1–45) to Z.N. We also gratefully acknowledge the support from Chulalongkorn University under Ratchadaphiseksomphot Endowment awarded to the Center of Excellence for Molecular Biology and Genomics of Shrimp.

AUTHOR CONTRIBUTIONS

A.T. contributed the conceptualization, supervision, and funding acquisition. A.T. and Z.N. contributed to the study, experimental designs, and funding acquisition. T.K. participated in the supervision, review of the study, collaboration, and provided a part of the resources. Z.N. performed *in vivo* and *in vitro* experiments and analyzed the data. A.T., T.K., and Z.N. reviewed the results, wrote, edited, and approved the final version of the manuscript.

DECLARATION OF INTERESTS

The authors declare no competing interests, and the research was conducted in the absence of any commercial or financial relationships that could be construed as a potential conflict of interest.

Received: September 24, 2023
Revised: January 15, 2024
Accepted: May 29, 2024
Published: May 31, 2024

REFERENCES

1. Chen, S.N., Gan, Z., Hou, J., Yang, Y.C., Huang, L., Huang, B., Wang, S., and Nie, P. (2022). Identification and establishment of type IV interferon and the characterization of interferon-υ including its class II cytokine receptors IFN-υR1 and IL-10R2. Nat. Commun. *13*, 999.
2. Janeway, C.A., and Medzhitov, R. (2002). Innate immune recognition. Annu. Rev. Immunol. *20*, 197–216.
3. Li, C., Li, H., Chen, Y., Chen, Y., Wang, S., Weng, S.-P., Xu, X., and He, J. (2015). Activation of Vago by interferon regulatory factor (IRF) suggests an interferon system-like antiviral mechanism in shrimp. Sci. Rep. *5*, 15078.
4. Levy, D.E., Marié, I.J., and Durbin, J.E. (2011). Induction and function of type I and III interferon in response to viral infection. Curr. Opin. Virol. *1*, 476–486.
5. Adams, M.D., Celniker, S.E., Holt, R.A., Evans, C.A., Gocayne, J.D., Amanatides, P.G., Scherer, S.E., Li, P.W., Hoskins, R.A., Galle, R.F., et al. (2000). The genome sequence of Drosophila melanogaster. Science *287*, 2185–2195.
6. Holt, R.A., Subramanian, G.M., Halpern, A., Sutton, G.G., Charlab, R., Nusskern, D.R., Wincker, P., Clark, A.G., Ribeiro, J.M.C., Wides, R., et al. (2002). The genome sequence of the malaria mosquito Anopheles gambiae. Science *298*, 129–149.
7. Kobayashi, M., Johansson, M.W., and Söderhäll, K. (1990). The 76 kD cell-adhesion factor from crayfish haemocytes promotes encapsulation *in vitro*. Cell *260*, 13–18.
8. Lee, S.Y., and Söderhäll, K. (2002). Early events in crustacean innate immunity. Fish Shellfish Immunol. *12*, 421–437.
9. Tassanakajon, A. (2013). Innate immune system of shrimp. Fish Shellfish Immunol. *34*, 953.
10. Kawai, T., and Akira, S. (2009). The roles of TLRs, RLRs and NLRs in pathogen recognition. Int. Immunol. *21*, 317–337.
11. Sabin, L.R., Hanna, S.L., and Cherry, S. (2010). Innate antiviral immunity in *Drosophila*. Curr. Opin. Immunol. *22*, 4–9.
12. Hinz, M., and Scheidereit, C. (2014). The IκB kinase complex in NF-κB regulation and beyond. EMBO Rep. *15*, 46–61.
13. Tassanakajon, A., Rimphanitchayakit, V., Visetnan, S., Amparyup, P., Somboonwiwat, K., Charoensapsri, W., and Tang, S. (2018). Shrimp humoral responses against pathogens: antimicrobial peptides and melanization. Dev. Comp. Immunol. *80*, 81–93.
14. Wang, P.H., Gu, Z.H., Wan, D.H., Liu, B.D., Huang, X.D., Weng, S.P., Yu, X.Q., and He, J.G. (2013). The shrimp IKK-NF-κB signaling pathway regulates antimicrobial peptide expression and may be subverted by white spot syndrome virus to facilitate viral gene expression. Cell. Mol. Immunol. *10*, 423–436.
15. Amaya, M., Keck, F., Bailey, C., and Narayanan, A. (2014). The role of the IKK complex in viral infections. Pathog. Dis. *72*, 32–44.
16. Nhnhkorn, Z., Amparyup, P., Kawai, T., and Tassanakajon, A. (2019). *Penaeus monodon* IKKs participate in regulation of cytokine-like system and antiviral responses of innate immune system. Front. Immunol. *10*, 1430.
17. Boonchuen, P., Sakhor, H., Jaree, P., and Somboonwiwat, K. (2022). Shrimp Vago5 activates an innate immune defense upon bacterial infection. Fish Shellfish Immunol. *120*, 122–132.

18. Paradkar, P.N., Trinidad, L., Voysey, R., Duchemin, J.-B., and Walker, P.J. (2012). Secreted Vago restricts West Nile virus infection in *Culex* mosquito cells by activating the Jak-STAT pathway. Proc. Natl. Acad. Sci. USA *109*, 18915–18920.
19. Li, F., and Xiang, J. (2013). Signaling pathways regulating innate immune responses in shrimp. Fish Shellfish Immunol. *34*, 973–980.
20. Bakshi, S., Taylor, J., Strickson, S., McCartney, T., and Cohen, P. (2017). Identification of TBK1 complexes required for the phosphorylation of IRF3 and the production of interferon β. Biochem. J. *474*, 1163–1174.
21. Schneider, J., and Imler, J.-L. (2021). Sensing and signalling viral infection in drosophila. Dev. Comp. Immunol. *117*, 103985.
22. Ware, J., and Varughese, K.I. (2017). Structural origins of hemostasis and adaptive immunity. Res. Pract. Thromb. Haemost. *1*, 286–290.
23. Qin, N., Sun, H., Lu, M., Wang, J., Tang, T., and Liu, F. (2020). A single von Willebrand factor C-domain protein acts as an extracellular pattern-recognition receptor in the river prawn *Macrobrachium nipponense*. J. Biol. Chem. *295*, 10468–10477.
24. Gao, J., Zhao, B.-R., Zhang, H., You, Y.-L., Li, F., and Wang, X.-W. (2021). Interferon functional analog activates antiviral Jak/Stat signaling through integrin in an arthropod. Cell Rep. *36*, 109761.
25. Paradkar, P.N., Duchemin, J.-B., Voysey, R., and Walker, P.J. (2014). Dicer-2-dependent activation of *Culex* vago cccurs via the TRAF-Rel2 signaling pathway. PLoS Neglected Trop. Dis. *8*, e2823.
26. Limkul, S., Phiwthong, T., Massu, A., Jaree, P., Thawonsuwan, J., Teaumroong, N., Boonanuntanasarn, S., Somboonwiwat, K., and Boonchuen, P. (2022). The interferon-like proteins, Vagos, in *Fenneropenaeus merguiensis* elicit antimicrobial responses against WSSV and VPAHPND infection. Fish Shellfish Immunol. *131*, 718–728.
27. Potapova, I.A., Cohen, I.S., and Doronin, S.V. (2010). Von willebrand factor increases endothelial cell adhesiveness for human mesenchymal stem cells by activating p38 mitogen-activated protein kinase. Stem Cell Res. Ther. *1*, 35.
28. Eleftherianos, I., Heryanto, C., Bassal, T., Zhang, W., Tettamanti, G., and Mohamed, A. (2021). Haemocyte-mediated immunity in insects: Cells, processes and associated components in the fight against pathogens and parasites. Immunology *164*, 401–432.
29. Asad, S., Parry, R., and Asgari, S. (2018). Upregulation of *Aedes aegypti* Vago1 by *Wolbachia* and its effect on dengue virus replication. Insect Biochem. Mol. Biol. *92*, 45–52.
30. Mussabekova, A., Daeffler, L., and Imler, J.-L. (2017). Innate and intrinsic antiviral immunity in *Drosophila*. Cell. Mol. Life Sci. *74*, 2039–2054.
31. Macke, A., Lopez, W., Carlson, D.J., and Carlson, K.A. (2020). Nora virus VP4b and ORF1 circulate in hemolymph of infected *D. melanogaster* with coordinate expression of Vago and Vir-1. Vaccines *8*, 491.
32. Xu, J., and Cherry, S. (2014). Viruses and antiviral immunity in *Drosophila*. Dev. Comp. Immunol. *42*, 67–84.
33. Soponpong, S., Amparyup, P., Kawai, T., and Tassanakajon, A. (2021). *Penaeus monodon* interferon regulatory factor (*Pm*IRF) activates IFNs and antimicrobial peptide expression via a STING-dependent DNA sensing pathway. Front. Immunol. *12*, 818267.
34. Ertürk-Hasdemir, D., Broemer, M., Leulier, F., Lane, W.S., Paquette, N., Hwang, D., Kim, C.-H., Stöven, S., Meier, P., and Silverman, N. (2009). Two roles for the *Drosophila* IKK complex in the activation of Relish and the induction of antimicrobial peptide genes. Proc. Natl. Acad. Sci. USA *106*, 9779–9784.
35. Häcker, H., and Karin, M. (2006). Regulation and function of IKK and IKK-related kinases. Sci. STKE *2006*, re13.
36. Descargues, P., Sil, A.K., and Karin, M. (2008). IKKalpha, a critical regulator of epidermal differentiation and a suppressor of skin cancer. EMBO J. *27*, 2639–2647.
37. Harris, J., Olière, S., Sharma, S., Sun, Q., Lin, R., Hiscott, J., and Grandvaux, N. (2006). Nuclear accumulation of cRel following C-terminal phosphorylation by TBK1/IKK epsilon. J. Immunol. *177*, 2527–2535.
38. Supungul, P., Tang, S., Maneeruttanarungroj, C., Rimphanitchayakit, V., Hirono, I., Aoki, T., and Tassanakajon, A. (2008). Cloning, expression and antimicrobial activity of crustin*Pm*1, a major isoform of crustin, from the black tiger shrimp *Penaeus monodon*. Dev. Comp. Immunol. *32*, 61–70.
39. Arayamethakorn, S., Supungul, P., Tassanakajon, A., and Krusong, K. (2017). Characterization of molecular properties and regulatory pathways of Crustin*Pm*1 and Crustin*Pm*7 from the black tiger shrimp *Penaeus monodon*. Dev. Comp. Immunol. *67*, 18–29.
40. Kamsaeng, P., Tassanakajon, A., and Somboonwiwat, K. (2017). Regulation of antilipopolysaccharide factors, ALF*Pm*3 and ALF*Pm*6, in *Penaeus monodon*. Sci. Rep. *7*, 12694.
41. Wang, P.-H., Gu, Z.-H., Huang, X.-D., Liu, B.-D., Deng, X.-X., Ai, H.-S., Wang, J., Yin, Z.-X., Weng, S.-P., Yu, X.-Q., et al. (2009). An immune deficiency homolog from the white shrimp, *Litopenaeus vannamei*, activates antimicrobial peptide genes. Mol. Immunol. *46*, 1897–1904.
42. Feng, N., Wang, D., Wen, R., and Li, F. (2014). Functional analysis on immune deficiency (IMD) homolog gene in Chinese shrimp *Fenneropenaeus chinensis*. Mol. Biol. Rep. *41*, 1437–1444.
43. Amparyup, P., Charoensapsri, W., and Tassanakajon, A. (2013). Prophenoloxidase system and its role in shrimp immune responses against major pathogens. Fish Shellfish Immunol. *34*, 990–1001.
44. Cerenius, L., and Söderhäll, K. (2004). The prophenoloxidase-activating system in invertebrates. Immunol. Rev. *198*, 116–126.
45. Visetnan, S., Supungul, P., Hirono, I., Tassanakajon, A., and Rimphanitchayakit, V. (2015). Activation of *Pm*Relish from *Penaeus monodon* by yellow head virus. Fish Shellfish Immunol. *42*, 335–344.
46. Pfaffl, M.W. (2001). A new mathematical model for relative quantification in real-time RT-PCR. Nucleic Acids Res. *29*, e45.

STAR★METHODS

KEY RESOURCES TABLE

REAGENT or RESOURCE	SOURCE	IDENTIFIER
rowheadAntibodies		
Mouse monoclonal anti 6x-His tag (HIS.H8)	Thermo Fisher	Cat# MA1-21315; RRID: AB_557403
Mouse monoclonal anti-Myc Taq, clone 9E10	Sigma-Aldrich	Cat# 630731; RRID: AB_2313773
Rabbit monoclonal anti-β tubulin	Abcam	Cat# ab179513; RRID: AB_3073861
Rabbit polyclonal anti-VWDE	Merck	Cat# HPA026619; RRID: AB_2671920
Mouse monoclonal anti-VWF (clone VWF/1465)	Abcam	Cat# ab218333; RRID: AB_2313773
Goat anti-mouse HRP	Abcam	Cat# ab6789; RRID: AB_955439
Goat anti-rabbit HRP	Abcam	Cat# ab6721; RRID: AB_95544
Goat anti-rabbit Alexa Fluor™ 568	Thermo Fisher	Cat# A78955; RRID: AB_2925778
Rabbit anti-mouse Alexa Fluor™ 488	Thermo Fisher	Cat# A27023; RRID: AB_2536087
rowheadBacterial and virus strains		
White spot syndrome virus	Lab isolated strain (Jaturontakul et al.[22])	N/A
Yellow head virus	Lab isolated strain (Visetnan et al.[23])	N/A
Vibrio parahaemolyticus AHPND	Lab isolated strain (Visetnan et al.[23])	N/A
Enterocytozoon hepatopenaei	Charoen Pokphand Foods PCL, Thailand	N/A
rowheadBiological samples		
Black tiger shrimp *Penaeus monodon*	Phetchaburi and Chachoengsao provinces, Thailand	N/A
Pacific white shrimp *Litopenaeus vannamei*	Charoen Pokphand Foods PCL, Thailand	N/A
Chemicals, peptides, and recombinant proteins		
Luna® Universal qPCR Master Mix	New England Biolabs	Cat# M3003L
DMEM, high glucose	Thermo Fisher	Cat# 11965092
Fetal Bovine Serum	Thermo Fisher	Cat# A4766801
Penicillin-Streptomycin	Thremo Fisher	Cat# 15140163
Lipofectamine™ 3000 Transfection Reagent	Thermo Fisher	Cat# L3000001
RIPA Lysis and Extraction Buffer	Thermo Fisher	Cat# 89900
DNaseI, RNase-free	New England Biolabs	Cat# EN0521
L-DOPA	Sigma	Cat# 59-92-7
Deposited data		
PmVago1	NCBI	GenBank: OQ730825
PmVaog2	NCBI	GenBank: OQ730826
PmVaog3	NCBI	GenBank: OQ730827
PmVago4	NCBI	GenBank: OQ730828
PmVaog5	NCBI	GenBank: OQ730829
Critical commercial assays		
SuperSignal™ West Pico PLUS Chemiluminescent Substrate	Thermo Fisher	Cat# 34577
Dual-Luciferase® Reporter Assay System	Promega	Cat# E1910
Experimental models: Cell lines		
HEK293T cell	Abcam	Cat# ab255449

(*Continued on next page*)

Continued

REAGENT or RESOURCE	SOURCE	IDENTIFIER
Oligonucleotides		
See Table S1 for a list of oligonucleotides	This paper	N/A
Software and algorithms		
GraphPad Prism 9	GraphPad Software	graphpad.com
Amersham Image Quant 800 Flour system	Cytiva	cytivalifesciences.com
ImageJ	NIH	ImageJ.net
SPSS Statistics	IBM	ibm.com
Other		
FavorPrep™ Tissue Total RNA Mini Kit	Favorgen	Cat# FATRK 001-2
FavorPrep™ Tissue Genomic DNA Extraction Mini Kit	Favorgen	Cat# FATGK 001-2
T7 RiboMAX™ Express Large Scale RNA Production System	Promega	Cat# P1320
RevertAid First Strand cDNA Synthesis Kit	Thermo Fisher	Cat# K1621

RESOURCE AVAILABILITY

Lead contact

Further information and requests for resources and reagents should be directed to and will be fulfilled by the Lead Contact, Anchalee Tassanakajon (anchalee.k@chula.ac.th).

Materials availability

This study did not generate new unique reagents.

Data and code availability

The raw sequencing data and all other data used for this study will be shared upon reasonable request from the lead contact.

The deposted sequence data for PmVagos are available in the NCBI database with the accession numbers within the deposited data section of the key resources table.

Any additional information required to reanalyze the data reported in this paper is available from the lead contact upon request.

EXPERIMENTAL MODEL AND STUDY PARTICIPANT DETAILS

Experimental shrimp and ethics statement

Healthy black tiger shrimp (*Penaeus monodon*, average body weight of 3–5 g each) were purchased from the local shrimp farms in Phetchaburi and Chachoengsao provinces, Thailand. They were tested for pathogen-free status by PCR with specific primers including WSSV, YHV, Vp_{AHPND}, and EHP (Table S1). For EHP infection experiment, the specific-pathogen free (SPF) Pacific white shrimp (*Litopenaeus vannamei*) with 3–5 g average body weight were obtained from the Marine Shrimp Broodstock Research Center II (MSBRC-2), Charoen Pokphand Foods PCL, Phetchaburi province, Thailand. The animals were fed with the commercial diet (Charoen Pokphand Foods PCL) at 5% of their body weight twice daily in a recirculating aquaria system filled with aerated sea water (20‰ salinity) at an ambient temperature 28 ± 1°C. They were cultivated in the new environment for at least 7 days for acclimation prior to experiments. This study was conducted according to the ethical principles and guidelines to animal use for scientific purposes by The National Research Council of Thailand (NRCT) and the protocol approved by Chulalongkorn University Animal Care and Use Committee (CU-ACUC) no. 2223002.

Preparation of shrimp pathogens

WSSV was prepared from the moribund WSSV-infected shrimp according to Jaturontakul et al., 2017. Briefly, shrimp were euthanized by iced-water immersion before gill collection and homogenization in TNE buffer (50 mM Tris-HCl pH 8.5, 400 mM NaCl, and 5 mM EDTA). The suspension was centrifuged at 3,500 × *g*, 4°C for 15 min and the supernatant was filtered through a 0.45-μm MILLEX-HP filter unit (Merck). The filtrate was centrifuged at 30,000 × *g*, 4°C for 30 min and the virion pellet was rinsed with TM buffer (50 mM Tris-HCl pH 7.5 and 10 mM $MgCl_2$). The virion suspension in TM buffer was centrifuged at 3,500 × *g* for 10 min at 4°C to remove the floating pellets. The WSSV pellet was resuspended in TM buffer and stored in −80°C until use.

YHV and *Vibrio parahaemolyticus* AHPND stocks were prepared as previously described.[45] For YHV stock preparation, gill was collected from the YHV-infected shrimp and ground in NTE buffer (0.02 M EDTA, 0.2 M NaCl, 0.2 M Tris-HCl, pH 6.5). The solution was filtered using a

0.45-μm MILLEX-HP filter unit (Merck) and centrifuged at 9000 × *g*, 4°C, 10 min. YHV solution stock was subsequently stored at −80°C until use. The virion numbers in WSSV and YHV stocks were determined by qRT-PCR and prepared for the infection at 1 × 10^5 copies. The infection virulence was 100% mortality within 10 days after infection for 3–4 g of juvenile shrimp.

Vibrio parahaemolyticus AHPND stock was prepared from bacterial culture in tryptic soy broth with OD_{600} at approximately 0.6. The colony forming unit (CFU) was determined by TCBS-agar plate counting and Vp_{AHPND} inoculum containing 1 × 10^5 CFU/mL was used for infection by immersion method.

For EHP infection experiment, healthy shrimp were cohabitated with EHP carrier shrimp to distribute the germinating EHP spore in aquaria. The preparation was done at the Marine Shrimp Broodstock Research Center II (MSBRC-2), Charoen Pokphand Foods PCL, Phetchaburi province, Thailand.

METHOD DETAILS

Nucleotide cloning and sequencing of *Vago* from *P. monodon*

The partial sequences of *P. monodon* Vago were retrieved by *in silico* searches from EST database (http://pmonodon.biotec.or.th) using query cDNA sequences from *L. vannamei* and genome BLAST against *P. monodon* reference genome (GenBank assembly accession no. GCA_015228065.1). The open reading frames of *PmVago1-5* were obtained by using gene specific nucleotide primers (Table S1) designed for PCR amplification and cDNA from shrimp hemocyte total RNA. In brief, the hemolymph was drawn in 1:1 ratio with cold modified Alserver's solution (MAS, 0.14 M NaCl, 0.1 M glucose, 30 mM trisodium citrate, 26 mM citric acid, 10 mM EDTA, pH 5.6) from shrimp ventral sinus and centrifuged at 800 × *g*, 4°C for 10 min for hemocyte separation. Total RNA was extracted for cDNA synthesis following manufacturer instructions described in FavorPrep Tissue Total RNA Mini Kit (Favorgen) and RevertAid First Strand cDNA Synthesis Kit (Thermo Scientific). PCR reactions were performed using 500 ng cDNA template equivalent to RNA amount in 50 μL of Q5 High-Fidelity DNA Polymerase (NEB) reaction volume. The PCR product fragments were cloned into pGEM-T Easy vector (Promega) for nucleotide sequencing (Macrogen).

Bioinformatics analysis

The amino acid sequences of *Pm*Vago1-5 were retrieved from the complete open reading frames translated by ExPASy Translate Tool (https://web.expasy.org/translate). Protein molecular weight (MW) and isoelectric point (pI) were predicted by Compute pI/Mw tool (https://web.expasy.org/compute_pi/). Multiple sequence alignment was performed in Clustal Omega (https://www.ebi.ac.uk/Tools/msa/clustalo) using deduced amino acid sequences of *Pm*Vago1-5 and other related species determined with BLAST algorithm at NCBI database (https://blast.ncbi.nlm.nih.gov/Blast.cgi). The putative functional protein motif features of Vagos were analyzed by Simple Modular Architecture Research Tool, SMART 9.0 (http://smart.embl-heidelberg.de). The phylogenetic tree was constructed based on the amino acid sequences of *Pm*Vago1-5 and related analogs from vertebrates and invertebrates including crustacean and arthropod species. The evolutionary relationship was determined using an unrooted neighbor-joining (NJ) method created by MEGA 11 software (http://www.megasoftware.net/index.html). The Bootstrap sampling iterations were 1000 times.

Tissue distribution analysis of *PmVago*

Gene expression of *PmVago1-5* was examined in *P. monodon* by semi-quantitative RT-PCR. Hemolymph was drawn in MAS solution as described above and centrifuged at 800 × *g*, 4°C, 10 min for hemocyte separation of prior to animal euthanasia by ice water immersion. Different tissues including gill, hepatopancreas, epipodite, muscle, stomach, intestine, eyestalk, heart, and lymphoid organ were collected and washed with phosphate buffered saline (1X PBS, pH7.4). The selected tissues were individually collected from three healthy shrimp for RNA extraction with FavorPrep Tissue Total RNA Mini Kit (Favorgen) and DNaseI (RNase-free) digestion (NEB). One microgram of total RNA templates was pooled and reversed transcribed in first strand cDNA synthesis using RevertAid First Strand cDNA Synthesis Kit (Thermo Scientific). The RNA extract and cDNA were stored in −80°C until use. PCR reactions were performed using 20 ng cDNA equivalent to RNA amount with specific forward and reverse primers (Table S1) in 25 μL of RBC *Tag* DNA polymerase (RBC Bioscience) reaction volume. The reactions were carried out according to manufacturer cycling protocol; 1 cycle of 94°C for 1 min followed by 30 cycles of 94°C for 30 s, 60°C for 30 s, and 72°C for 30 s. The final extension was 7 min at 72°C. Elongation factor-1α gene (*EF-1α*) was amplified for 25 cycles as an internal control. PCR products were analyzed by 2% (w/v) agarose-TBE gel electrophoresis and gel imaging UV-transilluminator.

Expression profiles of *PmVago1-5* in responses to viral, bacterial, and microsporidian challenges

To investigate the expression patterns of *PmVago1-5* in the hemocytes, shrimp immune responses were stimulated using disease causative microbial agents. Healthy *P. monodon* were injected intramuscularly in the third abdominal segment with 25 μL of phosphate buffered saline (1X PBS, 137mM NaCl, 2.7mM KCl, 4.3mM Na_2HPO_4, and 1.47mM KH_2PO_4, pH 7.4) as a control group. For microbial infection, shrimp were divided and injected with approximately 1×10^5 copies of purified WSSV, 1×10^5 copies of purified YHV or 1 × 10^5 CFU/mL of *V. parahaemolyticus* AHPND inoculum. Three shrimp from each group were randomly collected at 0, 6, 12, 24, 48 h post injection (hpi). For *Enterocytozoon hepatopenaei* (EHP) infection experiment, *L. vannamei* were cohabited for 15 days with carrier kindly given by Marine Shrimp Broodstock Research Center II (MSBRC-2), Charoen Pokphand Foods PCL, Thailand. Total hemocyte was sampled for

RNA isolation and cDNA synthesis. Quantitative RT-PCR analysis was performed using each sample prepared and pooled from three shrimp. The expression of *Pm*Vago1-5 in control group and immune-challenged shrimp was determined using 1 μL of cDNA template in 10 μL of Luna Universal qPCR Master Mix (NEB) reaction and 0.25 μM primer mix using CFX96 Touch Real-Time PCR Detection System (Bio-Rad). Primer sequences were listed in Table S1. The reaction was carried out in triplicate replications with the following cycling parameters; 1 cycle of 95°C for 1 min followed by 40 cycles of 95°C for 15 s and 60°C for 30 s. Melt curve analysis was performed at the end of thermal cycle for determining the specificity of amplification. The expression of *P. monodon* elongation factor-1α gene (*PmEF-1α*) was used as an internal control. The relative mRNA expression of *PmVago1-5* was calculated according to a comparative $2^{-\Delta\Delta Ct}$ method described by Pfaffl (2001). The data were shown as fold changes of means ± standard deviations (SD). Statistical analysis was performed using one-way ANOVA and Duncan's new multiple range test. The data was considered for statistical differences with the significance at $p < 0.05$.

Double-stranded RNA synthesis and *in vivo* suppression efficiency by dsRNA-Mediated RNA interference (RNAi)

Double-stranded RNA (dsRNA) specific to *PmVago1* (dsPmVago1), *PmVago4* (dsPmVago4), *PmVago5* (dsPmVago5), and *GFP* (dsGFP) genes were synthesized regarding *in vitro* transcription. Partial unique DNA fragment for target genes were amplified for sense and antisense RNA strand templates separately using specific primers linked with T7 RNA polymerase binding site (Table S1). The complementary single RNA strands were annealed and purified to generate dsRNAs as described in T7 RiboMAX Express RNAi System (Promega). A dsRNA targeting green fluorescence protein (dsGFP) for control group was synthesized from pEGFP-1 vector (Clonetech). Purified dsRNAs were quantified and stored at −80°C until use. To verify the *in vivo* suppression efficiency and the specificity of the dsRNAs, 5 μg/g shrimp body weight of either dsPmVago1, dsPmVago4, dsPmVago5 or dsGFP were injected into the third abdominal segment intramuscularly. The control group was injected with dsGFP. At 24 h post dsRNA injection, shrimp were infected with 1×10^5 copies of WSSV inoculum or PBS as the control. RNA interference was determined from shrimp hemocyte after 24 h post infection by qRT-PCR. The expression of elongation factor-1α gene (*EF-1α*) was used as an internal control. The experiment was carried out in triplicates.

Survival rates of *PmVago*-suppressed shrimp after WSSV infection

To further investigate the roles of *PmVago1*, *PmVago4*, and *PmVago5* upon WSSV infection, dsRNA-mediated RNAi followed by WSSV infection were performed. Shrimp were divided into 3 groups of 10 shrimp (4–5 g) for a type of dsRNA (30 total). They were injected with 5 μg/g shrimp of *in vitro*-transcribed dsGFP as a control, dsPmVago1+dsPmVago4 cocktail, and dsPmVago5 in 1X PBS. With an interval of 24h, shrimp were injected intramuscularly with 1×10^5 copies of purified WSSV or 150 mM NaCl as a control. The internal control was injected with dsGFP in PBS followed by 150 mM NaCl. The cumulative mortalities were recorded daily for a period of 10 days post WSSV infection. The experiment was carried out in the independent triplicates. The survival rates were statistically analyzed using one-way ANOVA with the significance at $p < 0.05$.

Quantification of WSSV copy number in *PmVago*-Suppressed shrimp

In order to monitor the WSSV copies, absolute quantitative PCR (qPCR) was conducted with the viral conserved *VP28* gene. Shrimp were divided and injected with dsGFP, dsPmVago1+dsPmVago4 cocktail, and dsPmVago5 in 1X PBS followed by 1×10^5 copies of purified WSSV. At the timepoints of 24, 72, 96 until 120h with approximately 50% cumulative mortality, grills were randomly sampled for genomic DNA extraction using FavorPrep Tissue Genomic DNA Extraction Mini Kit (Favorgen). Total genomic DNA was quantified by NanoDrop 2000c Spectrophotometer (Thermo Scientific) and used as the gDNA template for WSSV number quantification. Absolute qRT-PCR was performed in three replicates using Luna Universal qPCR Master Mix (NEB) with 10 ng total gDNA and *VP28* primers (Table S1). The cycling condition was performed with 1 cycle of 95°C, 1 min, followed by 40 cycles of 95°C for 15 s and 60°C for 30 s. The recombinant plasmid containing a conserved region of WSSV *VP28* gene was used to generate the 10-fold serial dilution internal standard. Statistical analysis was performed using one-way ANOVA with the significance at $p < 0.05$.

PmVago suppression effects on immune-related genes after WSSV infection

To examine *PmVago1*, *PmVago4*, and *PmVago5* suppression effects on immune-related genes, dsRNA-mediated RNAi was performed. Shrimp were separated and injected intramuscularly with 5 μg/g shrimp body weight of dsGFP for control, dsPmVago1+dsPmVago4 cocktail, and dsPmVago5 dissolved in 1X PBS. At 24h, shrimp were stimulated with 1×10^5 copies of purified WSSV inoculum or 1X PBS as a control. Five shrimp per group were randomly sampled at 24h post infection for total hemocyte RNA extraction and cDNA synthesis. The expression profiles of the major antimicrobial peptides involved in shrimp pathogen response against WSSV under Toll and IMD pathways were determined by qRT-PCR using specific primers (Table S1) including *ALFPm3*, *ALFPm6*, *CrustinPm1*, *CrustinPm5*, *CrustinPm7*, *PEN3*, and *PEN5*. The other immune-related genes included immune receptors (*Domeless*, *Toll*, *Integrin*), and signal transducers (*IKK*, *JAK*, *STAT*, *Cactus*, *Dorsal*, *Relish*, *Spätzle*, *IMD*, *MyD88*).

The reactions were performed in Luna Universal qPCR Master Mix (NEB) system with gene specific primers and 20 ng cDNA equivalent to RNA amount per 10 μL reaction volume. Quantitative RT-PCR was carried out in CFX96 Touch Real-Time PCR Detection System (Bio-Rad) with the following thermal cycles; 1 cycle of 95°C for 1 min followed by 40 cycles of 95°C for 15 s and 60°C for 30 s. The expression of elongation factor-1α gene (*EF-1α*) was used as an internal control. Melt curve analysis was performed at the end of PCR thermal cycle for determining the

specificity of amplification. The reactions were carried out in triplicates and the relative expression was calculated using a comparative method described by Pfaffl, 2001.[46] The data were shown as means ± standard deviations (SD). Statistical analysis was performed using one-way ANOVA followed by Duncan's new multiple range test. The data was considered for statistical differences with the significance at $p < 0.05$.

Prophenoloxidase activity assay in *PmVago1*-and *PmVago4*-suppressed shrimp

To investigate the RNAi effects of the most WSSV-responding *PmVago* on shrimp proPO system, PO activity was determined *in vitro* by measuring the oxidation of L-DOPA to dopachromes. At 24 h post dsRNA injection followed by WSSV infection, hemocyte lysate (HLS) from *Vago1*-and *Vago4*-suppressed shrimp was prepared. The total hemolymph was withdrawn into the 10 mM Tris-HCl pH8.8-containing insulin needles. For PO activation assay, the reaction was carried out in a clear 96-well plate. HLS (250 μg total protein) was added to the reaction containing 125 μL of 10 mM Tris-HCl pH8.8 followed by 25 μL of L-DOPA (3 mg/mL) substrate. Subsequently, 5 μL of LPS solution (0.1 mg/mL) was added to stimulate the reaction prior to incubation at room temperature for 30 min. The absorbance at 490 nm was measured using a spectrophotometer in clear 96-well plate.

Immunofluorescence microscopic detection of *Pm*Vago1 and *Pm*Vago4 in shrimp hemocytes

Protein expression and localization of *Pm*Vago1 and *Pm*Vago4 in shrimp hemocytes were analyzed upon WSSV infection by immunofluorescence staining. Shrimp were injected with WSSV inoculum (1×10^5 copies) to stimulate antiviral immune responses or 1X PBS for control. At 24 and 48 h post infection, WSSV loads were determined to verify the infectivity by qRT-PCR. To monitor protein localization, shrimp hemolymph was drawn and the hemocytes were fixed with 4% (w/v) paraformaldehyde in MAS solution (1:1 ratio). Total hemocytes were separated by 800 × *g*, 4°C, 10 min centrifugation and resuspended in 1X phosphate buffered saline (1X PBS, pH 7.4) before counting with a hemocytometer. Cells (1×10^5) were seeded onto poly-L-lysine coated coverslips in 24-well plates and washed three times with washing buffer (0.02% (v/v) TritonX-100 in 1X PBS, pH7.4). Cells were permeabilized with 100 mM glycine in 1X PBS containing 0.02% TritonX-100 for 30 min. Non-specific immunoprobing was blocked with 1X PBS containing 10% (w/v) FBS and 0.02% (v/v) TritonX-100 at 4°C for overnight. The endogenous *Pm*Vago1 and *Pm*Vago4 proteins were detected with 1:2000 rabbit anti-human VWDE (Merck, Germany) and 1:5000 mouse anti-VWF/1465 (Abcam, England) primary antibodies, respectively, in blocking buffer at at 4°C for overnight. The excess primary antibodies were wash for secondary antibodies probing. PmVago1 was labeled red with 1:5000 goat anti-rabbit secondary antibody conjugated with Alexa Fluor568 (Thermo Scientific), while PmVago4 was labeled in green with 1:5000 rabbit anti-mouse antibody conjugated with Alexa Fluor488 (Thermo Scientific) in blocking buffer. Samples were incubated for 1 h at RT, dark and the nuclei were stained with 1:2000 Hoechst 33342 (Thermo Scientific). The coverslips were mounted onto glass slides with Prolong Gold antifade reagent (Thermo Scientific) and sealed. Fluorescence microscopic images were visualized under laser scanning confocal microscope (Carl Zeiss LSM-700). The nuclear co-localization of *Pm*Vago1 and *Pm*Vago4 was analyzed with nuclei stained with Hochest33342 in hemocyte using WCIF ImageJ software. In brief, the picture was opened with Image-Color-Split channels. The unused channels were closed and Plugins-colocalization analysis-colocalization threshold was performed. The colocalization percentage of *Pm*Vago with Hochest33342-stained nuclei was calculated by the shared area of *Pm*Vago and nucleus divided by area of nucleus.

Immunodetection of *Pm*Vago protein in hemocytes

To detect *Pm*Vago protein, hemocytes from PBS control and WSSV challenged shrimp were collected at 48 hpi in MAS solution by 800 × *g*, 4°C, 10 min centrifugation. Cells were washed in MAS solution after hemolymph was removed followed by 1X PBS, pH 7.4 and lysed with RIPA lysis buffer (Thermo Fisher Scientific, CA, USA). Protein amount was quantified by Bradford method and hemocyte lysates with 50 μg total protein were loaded onto a 12.5% (w/v) SDS-PAGE for Western blotting. The membranes were primarily probed with the antibodies; 1: 5000 rabbit anti-human VWDE (Merck, Germany) for *Pm*Vago1, 1:5000 mouse anti-VWF/1465 (Abcam, England) for *Pm*Vago4, and 1:1000 rabbit anti β-tubulin monoclonal as the internal control. The secondary antibodies either goat anti-rabbit or goat anti-mouse IgG conjugated with HRP was used in the 1:10000 ratio. The immobilized proteins were detected using SuperSignal West Pico PLUS Chemiluminescent Substrate (Thermo Fisher Scientific, CA, USA) in the Amersham Image Quant 800 Flour system (GE Healthcare, OH, USA).

Cell culture and plasmid construction

HEK293T cells were purchased from CH3 BioSystems and cultured in Dulbecco's modified Eagle's medium (Invitrogen) supplemented with 10% fetal bovine serum (Invitrogen) at 37°C in a humidified 5% CO_2/95% air atmosphere. The open reading frames (ORF) coding PmVago1, PmVago4, *PmIKKβ*, *PmIKKε1*, and *PmIKKε2* were amplified from *P. monodon* hemocyte cDNA. The purified fragments were cloned into pcDNA3.1-*c*-Myc to generate expression plasmids for recombinant Myc-tagged proteins. The pGL3-basic backbone vector (Promega) was used for luciferase reporter construction. The fragments of promoter regions (−336 to +123) of *Pm*Vago1, (−338 to +253) of *Pm*Vago1, (−125 to to +55) of *Pm*Relish, and (−129 to +76) of *Pm*Dorsal were cloned from *P. monodon* hemocyte genomic DNA. Primer sequences were listed in Table S1. The insert fragments of all constructs were confirmed by nucleotide sequencing (Macrogen).

Dual luciferase reporter assay

To investigate the synergy of *Pm*Vago1 and *Pm*Vago4 with shrimp cytokine-like system and IKK-NF-κB signaling cascade, dual luciferase reporter assay was performed. HEK293T cells (5×10^4 cells/well) were seeded on 24-well. After 24 h cells were transiently co-transfected with 50 ng of pGL3-*PmVago1* or pGL3-*PmVago4* luciferase reporter plasmids and 1 μg of *Pm*IKK protein expression plasmids using Lipofectamine 2000 (Invitrogen) at a ratio of 1:3 (μg:μl) in Opti-MEM (Life Technologies).

To examine the regulatory effect of *Pm*Vago1 and *Pm*Vago4 on certain immune signal transducers, cells were co-transfected with 1 μg of *Pm*Vago protein expression plasmids and 50 ng of pGL3-*Relish* or pGL3-*Dorsal* luciferase reporter plasmids. Negative control group was transfected with empty plasmid. As an internal control, 10 ng of pRL-TK *Renilla* luciferase reporter plasmid was transfected simultaneously. At 24 h after transfection, cells were harvested and lysed for the assessment of protein expression. Activities of the firefly and *Renilla* luciferases were measured using Dual-Glo Luciferase Assay System (Promega) according to the manufacturer instruction. Luciferase activities were measured in opaque 96-well plate using a TriStar^2 LB 942 Modular Multimode Microplate Reader (Berthold). The data were obtained from experiments carried out in three independent replicates.

QUANTIFICATION AND STATISTICAL ANALYSIS

The experiments including qRT-PCR, cumulative mortality, dual luciferase assay, protein quantification, and PO activity were performed in triplicate. All the data were presented as the mean ± standard deviation (SD). Statistical analysis was calculated using one-way ANOVA. The Duncan's new multiple range test was performed for statistical significance comparison between groups of numerical data. The data was considered for statistical differences with the significance at $*p < 0.05$.